Journal of
Medicinal Chemistry

Article

Application of Bivalent Bioisostere Concept on Design and Discovery of Potent Opioid Receptor Modulators

Hongguang Ma, Samuel Obeng, Huiqun Wang, Yi Zheng, Mengchu Li, Abdulmajeed M Jali, David Stevens, William L Dewey, Dana E Selley, and Yan Zhang

J. Med. Chem., **Just Accepted Manuscript** • DOI: 10.1021/acs.jmedchem.9b01767 • Publication Date (Web): 29 Nov 2019

Just Accepted

is published by the American Chemical Society. 1155 Sixteenth Street N.W., Washington, DC 20036

Application of Bivalent Bioisostere Concept on Design and Discovery of Potent Opioid Receptor Modulators

*Hongguang Ma,† Samuel Obeng,† Huiqun Wang,† Yi Zheng,† Mengchu Li,† Abdulmajeed M. Jali,‡ David L. Stevens,‡ William L. Dewey,‡ Dana E. Selley,‡ Yan Zhang†,**

†Department of Medicinal Chemistry, School of Pharmacy, Virginia Commonwealth University, 800 E Leigh Street, Richmond, Virginia 23298, United States

‡Department of Pharmacology and Toxicology, Virginia Commonwealth University, 410 North 12th Street, Richmond, Virginia 23298, United States

* Corresponding author: Tel: +1 (804) 828-0021. E-mail address: yzhang2@vcu.edu (Y. Zhang).

Abstract

Here we described the structural modification of previously identified MOR antagonist NAN, a 6*α*-*N*-7′-indolyl substituted naltrexamine derivative, and its 6*β*-*N*-2′-indolyl substituted analogue INTA by adopting the concept of "bivalent bioisostere". Three newly prepared opioid ligands **25** (NBF), **31** and **38**, were identified as potent MOR antagonists both in vitro and in vivo. Moreover, these three compounds significantly antagonized DAMGO-induced intracellular calcium flux and displayed varying degree of inhibition on cAMP production. Furthermore, NBF produced much less significant withdrawal effects than naloxone in morphine-pelleted mice. Molecular modeling studies revealed that these bivalent bioisosteres may adopt similar binding modes in the MOR and the "address" portions of them may have negative or positive allosteric modulation effects on the function of their "message" portions compared with NAN and INTA. Collectively, our successful application of the "bivalent bioisostere concept" identified a promising lead to develop novel therapeutic agents toward opioid use disorder treatments.

Introduction

It has been several decades since opioid binding sites were initially investigated in the 1950s.[1] During this period of time, different types of opioid receptors have been pharmacologically designated and characterized.[2-5] Among them, three main types, the μ opioid receptor (MOR), the κ opioid receptor (KOR), and the δ opioid receptor (DOR), have been extensively studied.[6-8] As members of G protein-coupled receptor (GPCR) superfamily, opioid receptors are widely distributed in the central and peripheral nervous system,[9-11] and they exert critical functions not only in modulation of pain experience, but also in other physiological and pathophysiological processes.[12-20] It has been proven that activation of different types of opioid receptors can pose various biological effects.[21-25] Based on these observations, a considerable number of opioid agonists and antagonists have been developed with varying degree of success to treat different diseases.[26-28] Among them, MOR ligands with different degrees of selectivity and efficacy have received significant attention as they played critical roles in the treatment of opioid use disorder (OUD).[29,30]

The latest statistics show that OUD remains a major threat to human health with growing economic cost and considerable impact on the health care system. Particularly in the United States, it has become a national epidemic due to the illicit use of non-medical prescription opioids over the past decades. The annual number of overdose deaths in the United States, largely caused by opioids, have nearly increased four-fold from 2001 to 2016 and the opioids-related mortality rate has reached the highest level with an increasing of 11.4% in 2016,[31] underlying an urgent need of efficacious medications to treat side effects attributable to opioids.

Presently, the FDA-approved treatments for OUD include opioid agonists, such as methadone and buprenorphine, and opioid antagonists, such as naltrexone (Figure 1).[29,30] As a MOR full agonist, methadone possessed great efficacy for opioid addiction maintenance, however, the respiratory depression and long period of withdrawal symptom precipitation have largely compromised its therapeutic efficiency.[32] Similarly, buprenorphine, a MOR partial agonist, also suffered undesirable effects.[33] As for the opioid antagonist naltrexone, it did not produce side effects associated with opioid agonists. However, high dose of naltrexone primarily contributes to undesirable effects, which could be attributable to the interactions between naltrexone and the DOR or KOR.[34] Therefore, it is still imperative to develop highly potent and selective MOR ligands devoid of undesired side effects.

With a continuous endeavor on developing selective opioid receptor ligands, we have established a small molecule library, which is mainly designed based on the "message-address concept", by introducing various heterocyclic substituents onto the epoxymorphinan skeleton. From this library, several potent and highly selective MOR ligands have been identified and characterized as lead compounds in treating OUD.[35-42] More recently, introduction of an indole moiety at the 6-position of epoxymorphinan group resulted in a series of novel ligands, among which 17-cyclopropylmethyl-3,14β-dihydroxy-4,5α-epoxy-6α-(indole-7-

carboxamido)morphinan (NAN) acted as a potent MOR antagonist both in vitro and in vivo (Figure 1).[42] Interestingly, a structurally similar compound, 17-cyclopropylmethyl-3,14*β*-dihydroxy-4,5*α*-epoxy-6*β*-(indole-2-carboxamido)morphinan (INTA) was identified previously as a MOR full agonist (Figure 1).[43] Further molecular modeling studies revealed that INTA and NAN may be bitopic ligands in which their identical "message" portion, namely the epoxymorphinan moiety, may bind to the MOR orthosteric binding site in a similar fashion, while their indole rings, referred to as the "address" portion, may interact with different domains of the MOR allosteric binding site. These results indicated that even subtle changes of allosteric interactions may influence the functional activity of opioid ligands. In addition, it has been reported that bitopic ligands may possess favorable pharmacological properties, e.g., high affinity and selectivity, on their target receptors.[44-47] Based on these observations, we thus decided to conduct structural modification of the indole rings at the 6-position of epoxymorphinan skeleton in INTA and NAN to further explore their structure-activity relationship (SAR).

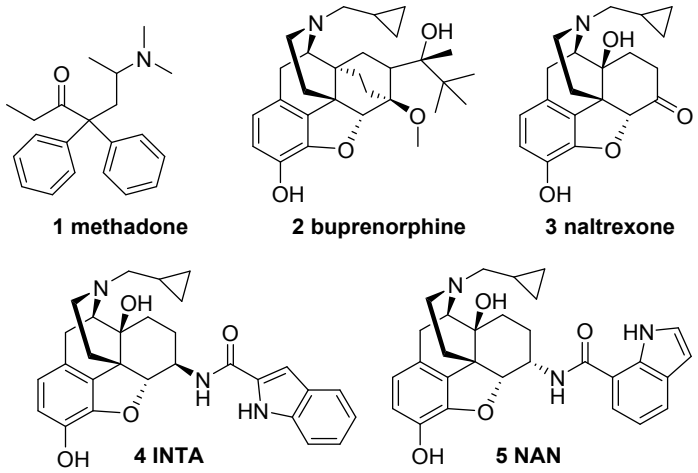

Figure 1. Chemical Structures of FDA-Approved Opioid Ligands, and NAN and INTA.

Since the concept of "bioisostere" was proposed by Harris Friedman in 1951,[48] the application of bioisosteres has become a tactical approach in drug design and lead optimization.[49] Among all bioisosteres, bivalent biososteres represented by -NH-, -O- and -S- moieties have been studied extensively because interchanges among them have facilitated identification of bioactive compounds.[50] Some of those representative applications are depicted in Figure 2. For example, the replacement of -NH- moiety in clozapine with -O- resulted in another marketed antipsychotic agent loxapine.[51,52] Further replacement of the oxygen atom in the loxapine skeleton with a sulfur atom led to approval of quetiapine in treating schizophrenia and other mental illnesses with favorable side-effect profile.[53]

Another successful application was found in a study of indolones derivatives (**9**−**11**).[54] Introduction of different bivalent bioisosteres resulted in retained inhibitory activities against cardiac phosphodiesterase, a potential target in the development of cardiotonic agent. In a study of adenosine 3',5'-cyclic phosphate

phosphodiesterase III (cAMP PDE III) inhibitors, introduction of -NH- and -O- moieties (compounds **12** and **13**) retained their inhibitory activities, while the sulfur derivative **14** showed greater potency for inhibition and turned out to be a more potent cardiotonic agent.[55] To summarize, numerous of studies have shown that the bioactivity of a specific bioisostere largely relies on the context, such as size, shape, polarity, electronegativity, and pKa, which potentially play critical roles in the molecule and target protein recognition.[50] To be noticed, introduction of bioisosteres may cause beneficial or deleterious effects while an effective bioisostere in one application may not be applicable in another case. Nevertheless, the application of bivalent bioisosteres is apparently a promising approach with significant value in drug design and discovery.

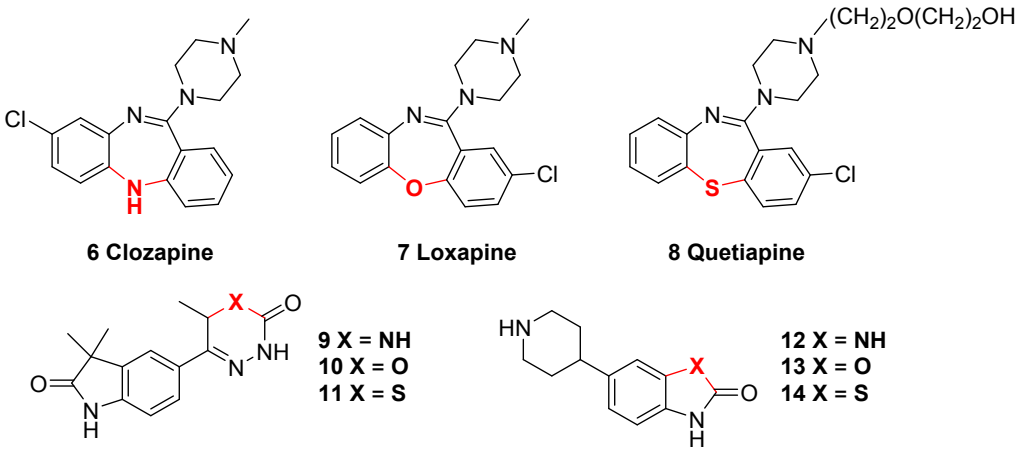

Figure 2. Representative Applications of Bivalent Bioisosteres.

We thus decided to apply the concept of "bivalent bioisostere" for the structural modification of INTA and NAN by replacing the -NH- moiety in indole ring with a -O- or -S- moiety, which resulted in two series of novel opioid ligands bearing benzofuran and benzothiophene moieties. In addition, complementary analogues in which an *α* and *β* amide linkages were also incorporated on different positions of heterocyclic substituents were also prepared in order to further understand the contributions of these structural changes to binding affinity and efficacy profiles at the MOR and the other two opioid receptors.

Results and Discussion

Chemical Synthesis. All newly designed compounds (except for two previously reported ones, compounds **15** and **16**)[43] were synthesized following previously reported procedure,[36,39,42] and the synthetic route is shown in Scheme 1. Briefly, using naltrexone as the start material, 6*α*- and 6*β*-naltrexamine were obtained under different stereoselective conditions with yield of 75% and 50%, respectively. Then various heterocyclic carboxylic acids, either purchased from commercial resources or prepared according to reported methods (see Supporting Information), reacted with 6*α*- or 6*β*-naltrexamine via EDCI/HOBt coupling reaction under mild

basic conditions. By treating with K_2CO_3 in methanol, the 6-monosubstitued free bases were obtained in reasonable yields. After transferring to hydrochloride salts, all target compounds were fully characterized and then submitted for biological studies.

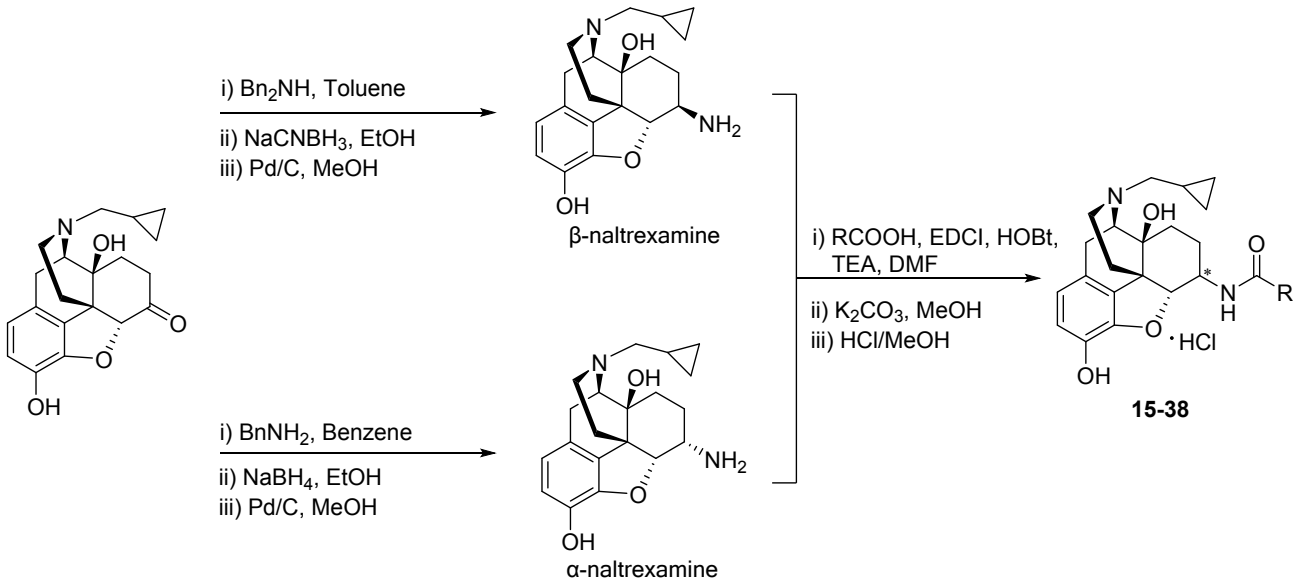

Scheme 1. Synthetic Route of Target Compounds Carrying Benzofuran and Benzothiophene Moieties.

In Vitro Pharmacological Studies. In order to characterize the binding affinity and selectivity of all newly synthesized ligands on the three opioid receptors, competitive radioligand binding assay was adopted on monoclonal mouse opioid receptor-expressed CHO cell membranes following reported protocol,[36,39,42] in which the MOR, DOR and KOR were labeled by [^{3}H]naloxone, [^{3}H]naltrindole, and [^{3}H]norBNI, respectively. The [^{35}S]-GTPγS functional assay was then carried out in an effort to characterize whether each ligand acted as a full agonist, partial agonist, or antagonist at the MOR as previously reported by measuring its relative efficacy to the full agonist DAMGO for MOR stimulation.[36]

As shown in Table 1, compounds **15**−**26** possessed subnanomolar binding affinity for the MOR and subnanomolar to nanomolar binding affinity at the KOR, while most of them bond to the DOR with low affinity of K_i value at two-digit nanomolar level, indicating that their opioid receptor selectivity profile was similar to that of INTA. In details, INTA exhibited low selectivity to the MOR over the KOR and DOR (K_i ratios $\kappa/\mu \approx 0.6$, $\delta/\mu \approx 5.3$), after replaced the -NH- of the indole ring with oxygen and sulfur atoms, no significant binding selectivity change in its counterparts compound **15** (K_i ratios $\kappa/\mu \approx 1.4$, $\delta/\mu \approx 12.1$) and compound **16** (K_i ratios $\kappa/\mu \approx 1.4$, $\delta/\mu \approx 9.9$) was observed. This result corroborated previously reported finding that compounds **15** and **16** afforded low selectivity in intracellular calcium release assay in human embryonic kidney 293 (HEK293) cells.[43] For other compounds, introduction of oxygen or sulfur atom appeared to have various effects on the selectivity of the MOR over the KOR and the DOR. For example, compounds **17** (K_i ratios $\kappa/\mu \approx 2.3$, $\delta/\mu \approx 79.2$) and **18** (K_i ratios $\kappa/\mu \approx 3.4$, $\delta/\mu \approx 133.21$) showed slightly improved selectivity for

the MOR over the KOR and the DOR in comparison with their bioisosteric counterpart bearing 3′-indolyl (K_i ratios $\kappa/\mu \approx 0.8$, $\delta/\mu \approx 37.7$).[42] While compound **21**(K_i ratios $\kappa/\mu \approx 1.4$, $\delta/\mu \approx 35.4$) and **22** (K_i ratios $\kappa/\mu \approx 1.5$, $\delta/\mu \approx 9.7$), in which the 5′-benzofuryl and 5′-benzothiophenyl were incorporated, respectively, at the 6-position of epoxymorphinan skeleton, possessed retained selectivity for the MOR over the KOR but relatively reduced selectivity for the MOR over the DOR compared with their corresponding bioisosteric counterpart (K_i ratios $\kappa/\mu \approx 2.0$, $\delta/\mu \approx 68.0$).[42]

Among the 6α-configuration analogues in Table 2, it was observed that the replacement of -NH- in the indole ring with oxygen and sulfur atoms resulted in retention of binding affinity at the MOR and the KOR and slightly increased selectivity of the MOR over the KOR and DOR (except for compounds **32**, **34** and **38**). Interestingly, NAN possessed moderate selectivity on the MOR over the KOR and DOR (K_i ratios $\kappa/\mu \approx 7.3$, $\delta/\mu \approx 59.5$), after -O- moiety was applied to replace the -NH- moiety, the resulting compound **37** showed higher selectivity with about 18-fold selectivity for the MOR over the KOR and about 104-fold selectivity for the MOR over the DOR. Introduction of a sulfur atom into the heterocyclic ring, however, somewhat retained selectivity of the MOR over the KOR but slightly decreased selectivity on the MOR over the DOR (compound **38**, K_i ratios $\kappa/\mu \approx 8.5$, $\delta/\mu \approx 26.9$). Additionally, it was also noticed that the different substituent positions of benzofuran and benzothiophene moieties seemed not to have very significant impact on MOR affinity and selectivity. That suggested that the "address" portion of these ligands in recognizing the MOR allosteric binding site was not influenced by the orientation of benzofuran and benzothiophene groups, which is consistent with our observations in INTA and NAN analogues.[42]

The [^{35}S]-GTPγS functional assay was then conducted using MOR-expressed CHO cell line as illustrated before.[36] As seen in Table 1, all target compounds primarily exhibited partial agonism with different levels of potency and efficacy. In details, INTA was known as a MOR full agonist, while among all 6β-configuration analogues, its bioisosteric counterparts, compounds **15** and **16** bearing 2′-benzofuryl and 2′-benzothiophenyl, respectively, turned out to be partial agonists with around 60% MOR stimulation. Meanwhile, it was also found that, after bivalent bioisosteric exchange, the efficacies of compounds **17** and **18** as well as compounds **23** and **24** were relatively decreased in comparison with their corresponding bioisosteric counterpart.[42] While the potencies and efficacies of compounds **21** and **22** (compound **21**, $EC_{50} = 0.41 \pm 0.02$ nM, $E_{max} = 52.23 \pm 1.42\%$; compound **22**, $EC_{50} = 0.19 \pm 0.03$ nM, $E_{max} = 75.43 \pm 2.30\%$) were largely increased compared to their bioisosteric counterpart carrying -NH- moiety ($EC_{50} = 2.98 \pm 1.25$ nM, $E_{max} = 22.32 \pm 3.50\%$).[42] For the rest of compounds, no obvious change in potency and efficacy was observed after bivalent bioisosteric replacement. Based on the functional assay results of target compounds with 6α-configuration, a trend was found that introduction of oxygen and sulfur atoms produced distinct reduction in MOR efficacy compared to corresponding -NH- counterpart (except for compound **35**).[42] Particularly, NAN has been identified as a MOR

antagonist as it had relative low efficacy of 19% compared to DAMGO. After -O- and -S- moieties were adopted to replace the -NH- moiety, the resulting counterparts **37** and **38** produced considerably lower efficacies (compound **37** E_{max} = 12.89 ± 1.78%; compound **38** E_{max} = 10.59 ± 0.93%). It demonstrated that the application of bivalent bioisosteres led to a beneficial impact on reducing the efficacy of NAN.

Previous observations have indicated that the configurational arrangement at 6-position of epoxymorphinan skeleton is critical for the affinity and selectivity of opioid receptor ligands,[56] which was also supported by our investigation regarding INTA and NAN series.[42] In the current study, comparisons were conducted in bioisosteric counterparts of INTA and NAN in an effort to further understand the impact of the stereochemistry at 6-position of the skeleton on ligand binding affinity and efficacy. Switching the linkage stereochemistry of counterparts of INTA, namely compounds **15** and **16**, from *β*-configuration to *α*-configuration (compounds **27** and **28**) did not change their MOR binding affinity but improved somewhat their selectivity on the MOR over the KOR and DOR (compound **15**, K_i ratios $\kappa/\mu \approx 1.4$, $\delta/\mu \approx 12.1$; compound **27**, K_i ratios $\kappa/\mu \approx 3.8$, $\delta/\mu \approx 81.6$; compound **16**, K_i ratios $\kappa/\mu \approx 1.4$, $\delta/\mu \approx 9.9$; compound **28**, K_i ratios $\kappa/\mu \approx 4.5$, $\delta/\mu \approx 53.0$). Meanwhile, distinct reductions in MOR efficacy were also observed. On the other hand, changing the linkage stereochemistry of compounds **37** and **38**, which are bioisosteric counterparts of NAN, from *α*-configuration to *β*-configuration (compounds **25** and **26**) did not lead to significant changes in MOR binding affinity, but had various effects on their selectivity profiles. Moreover, such changes in configuration also slightly increased their MOR efficacy. Collectively, our observations of the impact of the stereochemistry at 6-position of the epoxymorphinan skeleton on binding affinity and efficacy in bioisosteric counterparts of INTA and NAN were basically consistent with our previous results in INTA and NAN analogues.[42]

Table 1. The Binding Affinity, Selectivity, and MOR [^{35}S]-GTPγS Functional Assay Results of 6*β* Configuration Ligands Bearing Benzofuran and Benzothiophene Moieties. [a]

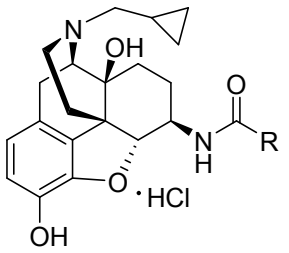

Compd	-R	K_i (nM)			Selectivity		MOR [^{35}S]-GTPγS binding	
		M	*K*	*δ*	*κ*/*μ*	*δ*/*μ*	EC_{50} (nM)	% E_{max} of DAMGO
4[b] (**INTA**)		0.29 ± 0.04	0.18 ± 0.00	1.54 ± 0.47	0.6	5.3	0.21 ± 0.01	92.42 ± 2.81
15		0.16 ± 0.02	0.23 ± 0.02	1.940 ± 0.37	1.4	12.1	0.39 ± 0.07	64.52 ± 1.41

16		0.14 ± 0.01	0.20 ± 0.02	1.39 ± 0.14	1.4	9.9	0.24 ± 0.03	59.05 ± 1.16
17		0.13 ± 0.01	0.30 ± 0.02	10.29 ± 2.53	2.3	79.2	0.47 ± 0.09	43.23 ± 2.00
18		0.14 ± 0.03	0.48 ± 0.06	18.65 ± 2.96	3.4	133.21	0.37 ± 0.05	29.91 ± 1.18
19		0.17 ± 0.03	0.80 ± 0.10	70.55 ± 10.60	4.7	415.0	0.59 ± 0.17	23.61 ± 1.29
20		0.16 ± 0.03	0.75 ± 0.08	24.04 ± 3.36	4.7	150.3	0.32 ± 0.06	23.06 ± 2.2
21		0.15 ± 0.03	0.21 ± 0.02	5.31 ± 1.05	1.4	35.4	0.41 ± 0.02	52.23 ± 1.42
22		0.14 ± 0.02	0.21 ± 0.03	1.36 ± 0.12	1.5	9.7	0.19 ± 0.03	75.43 ± 2.30
23		0.18 ± 0.03	0.30 ± 0.05	12.26 ± 2.53	1.7	68.1	0.59 ± 0.09	21.14 ± 1.33
24		0.15± 0.03	0.20 ± 0.01	2.04 ± 0.21	1.3	13.6	0.21 ± 0.02	58.71 ± 1.29
25 (NBF)		0.18 ± 0.03	0.81 ± 0.14	17.56 ± 3.17	4.5	97.6	0.95 ± 0.18	27.31 ± 3.26
26		0.19 ± 0.03	1.62 ± 0.18	38.93 ± 6.00	8.5	204.9	2.97 ±1.08	13.49 ± 1.94

[a]The values are the mean ± SEM of three independent experiments. [b]Data has been reported in Reference 42

Table 2. The Binding Affinity, Selectivity, and MOR [^{35}S]-GTPγS Functional Assay Results of 6α Configuration Ligands Bearing Benzofuran and Benzothiophene Moieties.[a]

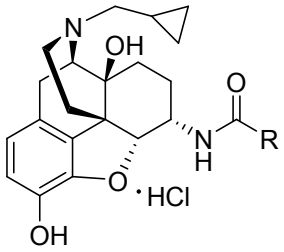

Compd	-R	K_i (nM)			Selectivity		MOR [^{35}S]-GTPγS binding	
		M	*K*	*δ*	*κ*/*μ*	*δ*/*μ*	EC_{50} (nM)	% E_{max} of DAMGO
5[b] **(NAN)**		0.23 ± 0.02	1.69 ± 0.35	13.69 ± 1.39	7.3	59.5	3.85 ± 2.32	19.11 ± 3.31
27		0.44 ± 0.04	1.67 ± 0.31	35.90 ± 9.90	3.8	81.6	5.52 ± 0.95	33.99 ± 1.45
28		0.27 ± 0.02	1.21 ± 0.10	14.31 ± 1.88	4.5	53.0	4.02 ± 0.85	22.91 ± 0.72
29		0.27 ± 0.04	3.37± 0.34	16.83 ± 3.35	12.5	62.3	1.57 ± 0.41	18.68 ± 0.65
30		0.20 ± 0.01	2.39 ± 0.19	9.07 ± 1.96	11.9	45.4	1.85 ± 0.37	14.26 ± 1.13
31		0.26 ± 0.04	4.98 ± 0.68	16.91 ± 2.10	19.2	65.0	0.77 ± 0.16	10.00 ± 0.48

32		0.26 ± 0.05	2.35 ± 0.49	6.85 ± 0.87	9.0	26.3	1.05 ± 0.26	16.09 ± 0.92
33		0.35 ± 0.03	4.23 ± 0.86	29.00 ± 5.46	12.1	82.9	3.72 ± 0.28	17.66 ± 0.63
34		0.39 ± 0.07	2.19 ± 0.28	11.87 ± 1.26	5.6	30.4	2.47 ± 0.36	18.88 ± 1.29
35		0.29 ± 0.03	1.66 ± 0.19	30.67 ± 3.83	5.7	105.8	2.23 ± 0.27	30.49 ± 2.19
36		0.28 ± 0.04	3.72 ± 0.67	22.28 ± 2.59	13.3	79.6	3.01 ± 0.68	18.11 ± 1.13
37		0.28 ± 0.04	5.12 ± 0.96	29.79 ± 4.60	18.3	106.4	0.97 ± 0.19	12.89 ± 1.78
38		0.31 ± 0.04	2.65 ± 0.32	8.35 ± 0.99	8.5	26.9	6.21 ± 2.08	10.59 ± 0.93

[a]The values are the mean ± SEM of three independent experiments. [b]Data has been reported in Reference 42

Molecular Modeling Study. As described above, INTA, compounds **15** and **16** (Figure S1) acted as partial agonists with around 60% MOR stimulation. NAN, compounds **37** and **38** (Figure S1) acted as antagonists produced low efficacies to the MOR. In order to understand the effects of bioisosteres on the binding modes of these compounds with the MOR, GOLD 5.6[57] was applied to dock INTA and its bioisosteric counterparts (compounds **15** and **16**) into the crystal structure of the agonist-bound (PDB ID: 5C1M) MOR.[58] Meanwhile, NAN and its bioisosteric counterparts (compounds **37** and **38)** were docked into the crystal structure of antagonist-bound (PDB ID: 4DKL) MOR.[59] The docking poses with the highest CHEM-PLP score were selected as the optimal binding poses of each compound, namely INTA-MOR^{active}, Compound 15-MOR^{active}, Compound 16-MOR^{active}, NAN-MOR^{inactive}, Compound 37-MOR^{inactive} and Compound 38-MOR^{inactive}, respectively. These six optimal binding poses were energy-minimized by a 10,000-iterations minimization in Sybyl-X 2.0 and displayed in Figures 3 and 4.

Comparing the chemical structures of INTA, NAN, and compounds **15**, **16**, **37**, and **38**, their "message" portions (epoxymorphinan moiety) are identical. Similar to INTA and NAN, the "message" portions of compounds **15**, **16**, **37**, and **38** also interacted with the MOR orthosteric binding site.[42] The ionic interactions with D$^{3.32}$ (superscript numbers follow the Ballesteros-Weinstein numbering method for GPCRs[60]), hydrogen bond interactions with Y$^{3.33}$, and hydrophobic interactions with residues M$^{3.36}$, W$^{6.48}$, and H$^{6.52}$ were observed with the "message" portion of each compound.

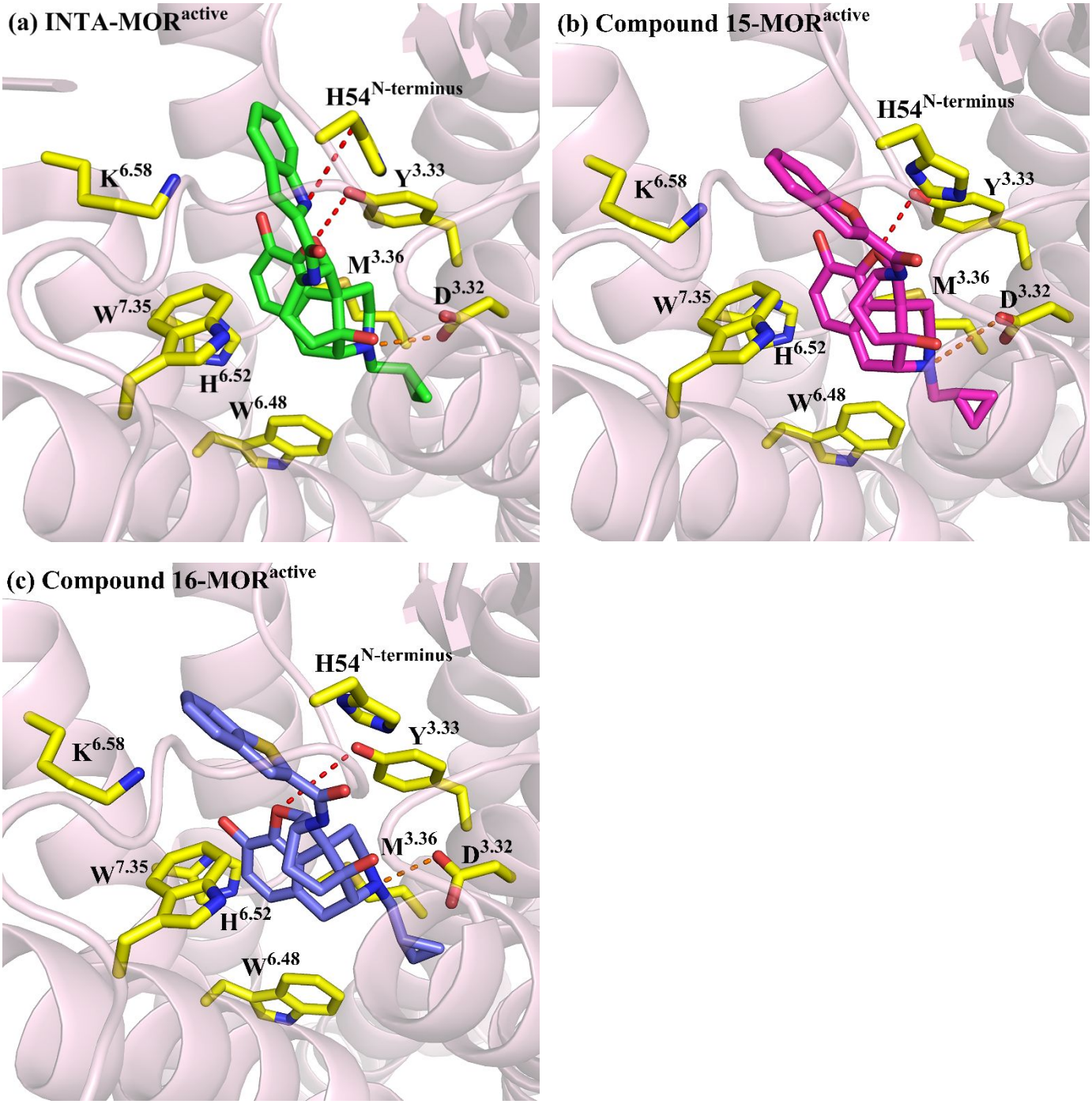

Figure 3. The binding modes of INTA-MOR^{active} (a), Compound 15-MOR^{active} (b), and Compound 16-MOR^{active} (c) from molecular docking studies. Protein shown as cartoon model in light-pink; INTA, compound **15**, compound **16**, and key amino acid residues shown as stick model. Carbon atoms: INTA (green), compound **15** (magentas), compound **16** (blue), key amino acid residues (yellow), oxygen atom (red), nitrogen atom (blue), sulfur atom (light-orange). The red dash line represents the hydrogen bond. The orange line represents the ionic interaction between D$^{3.32}$ and ligand. The inactive MOR crystal structure PDB ID, 4DKL.[59]

As reported in our previous study, the "address" portion of INTA formed hydrophobic interactions with H54$^{N\text{-terminus}}$ and π-π stacking interactions with W$^{7.35}$ located at the allosteric binding site.[42] Meanwhile, a hydrogen

bond existed between the -NH- moiety in indole ring of INTA and H54$^{N\text{-terminus}}$ (Figure 3 and Table S1). However, since the -NH- moiety in indole ring ("address" portion) of INTA was replaced by oxygen and sulfur atoms in compounds **15** and **16**, respectively, the hydrogen bond between the "address" portion of INTA and H54$^{N\text{-terminus}}$ didn't exist in Compound 15-MOR^{active} and Compound 16-MOR^{active} complexes. Hence, the "address" portions of compounds **15** and **16** were observed to have moved away from H54$^{N\text{-terminus}}$. Together with the effect of the larger atomic radius of sulfur atom,[61] the distance between the "address" portion of compound **16** and H54$^{N\text{-terminus}}$ was longer than that in INTA-MOR^{active} and Compound 15-MOR^{active} complexes. This movement may further cause the "address" portions of compounds **15** and **16** moved closer to W$^{7.35}$ (Table S1). Thus, the hydrophobic interactions with W$^{7.35}$ in Compound 15-MOR^{active} and Compound 16-MOR^{active} complexes seemed to be increased. Since the -NH- moiety in indole ring of INTA had direct interaction with H54$^{N\text{-terminus}}$ of MOR, changing the -NH- moiety in the "address" portion of INTA to -O- and -S- moieties may decrease the binding affinities of the "address" portions of compounds **15** and **16** with H54$^{N\text{-terminus}}$. However, due to the increase of the hydrophobic interactions with W$^{7.35}$ in Compound 15-MOR^{active} and Compound 16-MOR^{active} complexes, the binding affinities of INTA, compounds **15** and **16** in active MOR basically had no significant differences.

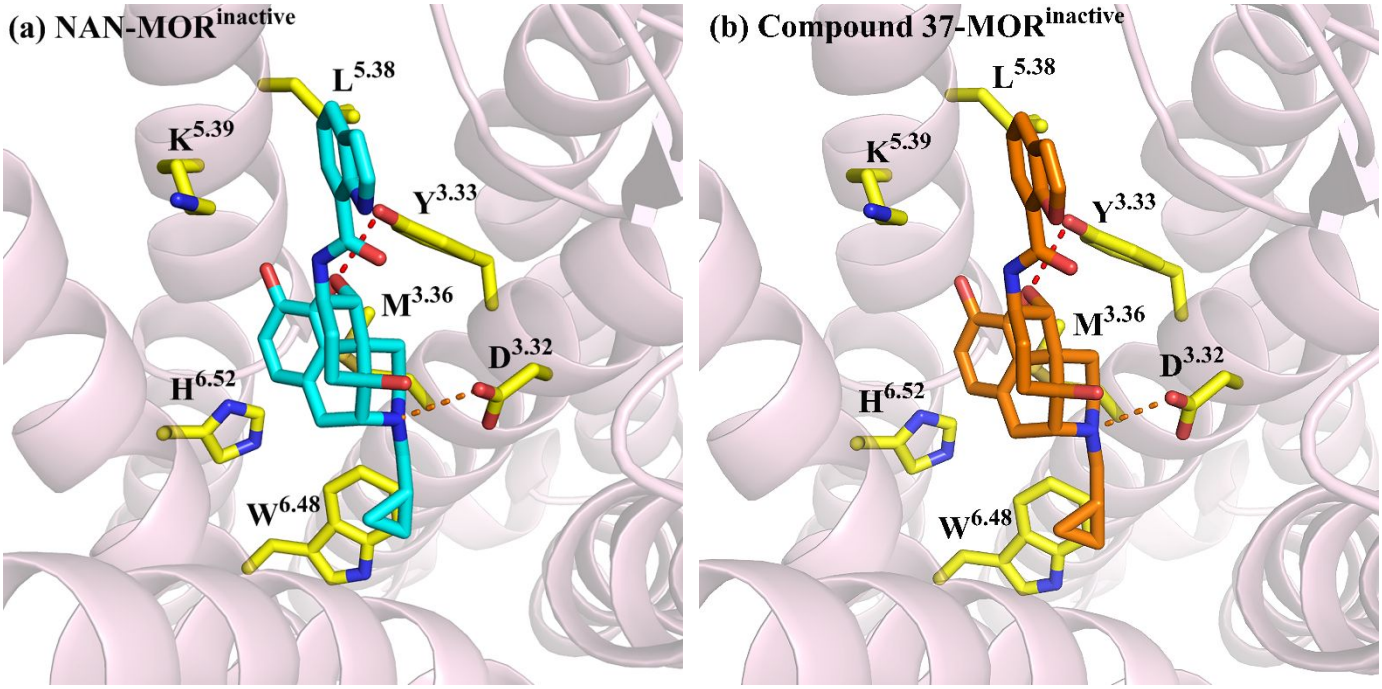

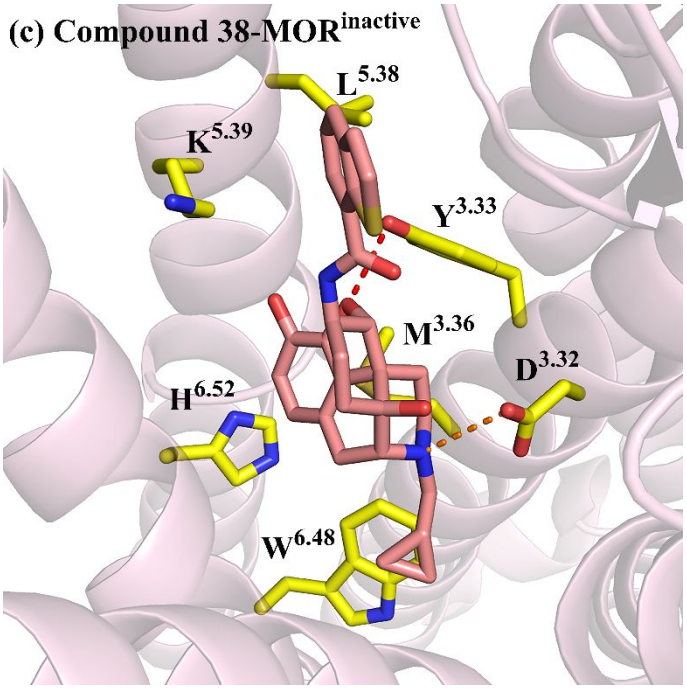

Figure 4. The binding modes of NAN-MOR^{inactive} (a), Compound 37-MOR^{inactive} (b), and Compound 38-MOR^{inactive} (c) from molecular docking studies. Protein shown as cartoon model in light-pink; NAN, compound **37**, compound **38**, and key amino acid residues shown as stick model. Carbon atoms: NAN (cyan), compound **37** (orange), compound **38** (pink), key amino acid residues (yellow), oxygen atom (red), nitrogen atom (blue), sulfur atom (light-orange). The red dash line represents the hydrogen bond. The orange line represents the ionic interaction between $D^{3.32}$ and ligand. The active MOR crystal structure PDB ID, 5C1M.[58]

From Figure 4, the binding modes of the "address" portions of NAN, compounds **37** and **38** were very similar. As described in our previous studies, the binding subdomain of the "address" portion of NAN shifted from $K^{6.58}$ and $W^{7.35}$ to $L^{5.38}$ and $K^{5.39}$ after 10 ns MD simulations. The "address" portion of NAN formed hydrophobic interactions with $L^{5.38}$ and $K^{5.39}$.[42] In the case of compounds **37** and **38**, it showed that the "address" portions of compounds **37** and **38** also formed hydrophobic interactions with $L^{5.38}$ and $K^{5.39}$ (Figure 4 and Table S1). Moreover, the distances listed in Table S1 suggested that the hydrophobic interactions with $L^{5.38}$ and $K^{5.39}$ in NAN-MOR^{inactive}, Compound 37-MOR^{inactive} and Compound 38-MOR^{inactive} complexes were almost the same. Since the -NH- moiety in indole ring of NAN had no direct interaction with MOR, bivalent bioisosteric exchange in the "address" portion of NAN from -NH- moiety to -O- and -S- moieties showed no significant effects on the binding of NAN, compounds **37** and **38** with inactive MOR.

In addition, the binding of the "address" portions of compounds **15** and **16** with $W^{7.35}$ at the allosteric binding site may cause the "message" portions of compounds **15** and **16** to form favorable interactions with $W^{6.48}$ (Table S1) to further stabilize the conformation of MOR in an active state. Such positive modulation effects of the "address" portions of compounds **15** and **16** were similar to that of INTA.[42] On the other hand, the hydrophobic interactions between residues $L^{5.38}$ and $K^{5.39}$ and the "address" portions of compounds **37** and **38**

may cause the "message" portions of compounds **37** and **38** away from $W^{6.48}$ (Table S1).[42] In consequence, the binding of the "message" portions with the orthosteric binding site weakened. Therefore, the "address" portions of compounds **37** and **38** may induce negative modulation effects on the function of the "message" portions of compounds **37** and **38**, which were similar to that of NAN.[42] Collectively, the benzofuran and benzothiophene moieties of compounds **15** and **16** seemed to exert the same function as that of a positive allosteric modulator (PAM), while the benzofuran and benzothiophene moieties of compounds **37** and **38** seemed to carry the same function as that of a negative allosteric modulator (NAM) at the MOR.

Additionally, INTA, NAN and compounds **15**, **16**, **37**, **38** were also docked into the KOR and DOR to compare their selectivity to the MOR over the KOR and DOR (Figures S2 and S3).[62-64] Similar to the six compounds binding with the MOR, their "message" portions interacted with the orthosteric binding sites of the KOR and DOR. The ionic interactions with $D^{3.32}$, hydrogen bond interactions with $Y^{3.33}$, and hydrophobic interactions with residues $M^{3.36}$, $W^{6.48}$, and $H^{6.52}$ were formed between the six compounds and the KOR and DOR. Meanwhile, in the KOR and DOR, their "address" portions binding with the same domain as those of the six compounds binding with the MOR. However, as some residues located at the allosteric binding sites among the three receptors were non-conserved ($L^{5.38}$, $K^{6.58}$, and $W^{7.35}$ in the MOR; $M^{5.38}$, $K^{6.58}$, and $Y^{7.35}$ in the KOR; and $T^{5.38}$, $W^{6.58}$, and $L^{7.35}$ in the DOR), the interactions between the "address" portions of the six compounds and the allosteric binding sites of the three receptors showed some differences. For INTA, compounds **15** and **16**, their "address" portions mainly formed hydrophobic interactions with $K^{6.58}$ and $W^{7.35}$ of the KOR and $W^{6.58}$ and $L^{7.35}$ of the DOR, which was similar to their binding with $K^{6.58}$ and $W^{7.35}$ of the MOR. For NAN, compounds **37** and **38**, their "address" portions formed hydrophobic interactions with $M^{5.38}$ and $K^{5.39}$ of the KOR and $T^{5.38}$ and $K^{5.39}$ of the DOR. As the hydrophobicity of $L^{5.38}$ in the MOR, $M^{5.38}$ in the KOR, and $T^{5.38}$ in the DOR was $L^{5.38} > M^{5.38} > T^{5.38}$, the hydrophobic interactions between the "address" portions of NAN, compounds **37** and **38** and the allosteric binding site of the three receptors was MOR > KOR > DOR. Thus, the similar interactions between INTA, compounds **15** and **16** with the MOR, KOR, and DOR may explain why these three compounds displayed no selectivity to the MOR, KOR and DOR. The different hydrophobic interactions between the "address" portions of NAN, compounds **37** and **38** with the allosteric binding site of the MOR, KOR and DOR may lead to certain degree of selectivity of NAN, compounds **37** and **38** to the MOR, KOR, and DOR.

In Vivo Warm-Water Tail Immersion Assay. Warm-water tail immersion assay was then conducted to examine the ability of each ligand to elicit antinociception or to antagonize the antinociception of morphine in mice as previously reported.[36] As seen in Figure 5A and 5B, compounds **15**, **16**, **21**, **22**, **23** and **24** (10 mg/kg) produced comparable percentage of maximum possible effect (% MPE) values as morphine, indicating

that these six compounds acted as agonists in vivo. Figure 5C depicted the potency of each ligand at 10 mg/kg to antagonize the antinociceptive effect of morphine at 10 mg/kg. As shown, compounds **19**, **25** (NBF), **27**, **29**, **31**, **33** and **38** were found to be potent antagonists of morphine and the other nine analogues had marginal to moderate impact on the antinociceptic effect of morphine. Dose response studies showed (Table 3) that compounds **19**, **27**, **29** and **33** possessed AD_{50} values ranging from 2.03 mg/kg to 3.21 mg/kg while compounds **31** and **38** carried greater potencies (AD_{50} values of 0.29 mg/kg) in comparison with NAN (AD_{50} = 2.07 mg/kg).[42] More notably, the AD_{50} value of NBF was determined as 0.18 mg/kg, which is 12-fold more potent compared to NAN.

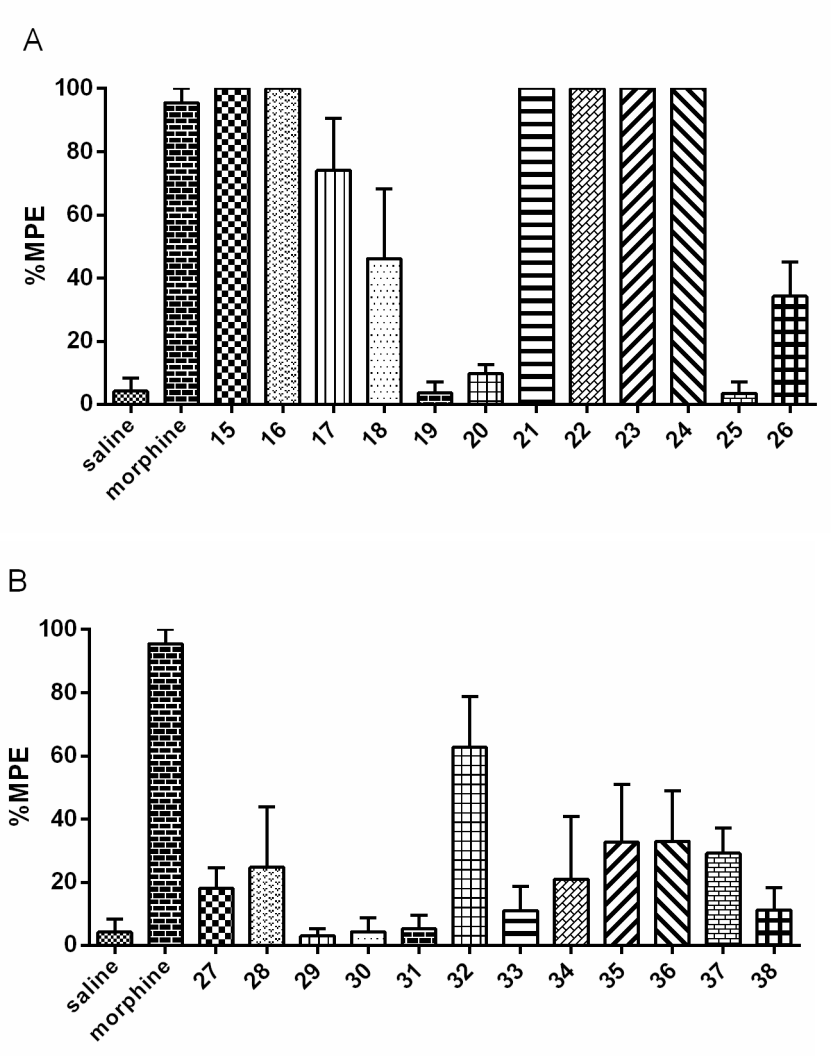

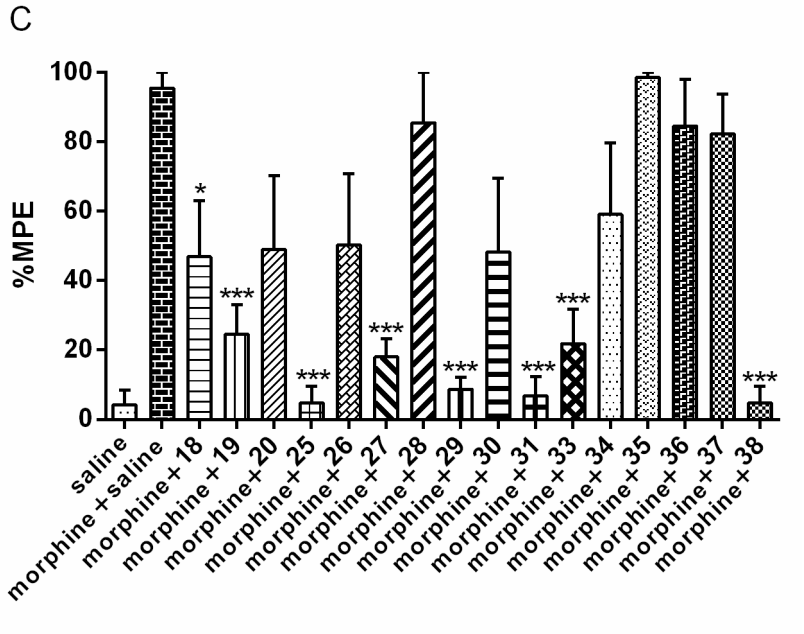

Figure 5. Warm-water tail immersion assay of synthesized analogues in mice (n = 5) at 56 ± 0.1 °C. All tested compounds were administered subcutaneously. (A) Antinociceptive effects of compounds **15-26** (10 mg/kg). (B) Antinociceptive effects of compounds **27-38** (10 mg/kg). (C) Blockage of the morphine-mediated antinociception of selected compounds (10 mg/kg) in the presence of morphine (10 mg/kg). Saline and morphine were adopted as negative and positive controls. Data are presented as mean values ± SD. ∗ indicates $P < 0.05$; ∗∗∗ indicates $P < 0.005$.

Table 3. AD_{50} Values of Selected Compounds to Antagonize Morphine-mediated Antinociception in Warm-Water Tail Immersion Assay in Vivo.

Compound	AD_{50} values (mg/kg (95% CL))
5 (NAN)[a]	2.07 (0.40-10.74)
19	2.79 (1.75-4.43)
25 (NBF)	0.18 (0.03-0.97)
27	3.21 (1.50-6.85)
29	2.51 (1.36-4.62)
31	0.29 (0.25-0.34)
33	2.03 (0.70-5.88)
38	0.29 (0.23-0.37)

[a]Data has been reported in Reference 42.

Calcium Flux Assay. It has been reported that the activation of G_q G-protein/calcium pathway may result in the rapid and transient increase of cytosolic calcium concentration.[65] Calcium flux measurement has become a key approach to evaluate GPCR function. To further profile three selected potent antagonists, NBF, compounds **31** and **38** in this G-protein mediated signaling cascade, calcium flux assay was conducted

following previously reported procedure.[66] The results suggested that all three tested compounds displayed no apparent agonism to increase intracellular calcium concentration (Figure 6A). On the other hand, all three of them concentration-dependently antagonized DAMGO-induced calcium flux (Figure 6B). In details, compound **38** was equipotent with the MOR antagonist naltrexone with IC_{50} value of 15.59 ± 1.96 nM, while compounds **31** and NBF showed lower potencies with IC_{50} values of 50.7 ± 2.88 nM and 566.14 ± 7.68 nM, respectively. The lack of agonism of these three compounds could be attributable to several factors. Firstly, the adoption of chimeric $G_{\alpha qi5}$ to transfect mMOR-CHO cells may result in such a phenomenon. Actually, similar results was also observed in 5-HT_{1A} receptor agonist ipsapirone, which efficaciously inhibited adenylyl cyclase (AC) activity but did not display any agonism in calcium flux assay.[67] Secondly, compounds **31** and **38** may act as neutral MOR antagonists in this signaling pathway according to their very low efficacy in GTPγS functional assay. As for NBF, it may behave similarly to compounds **31** and **38**, although NBF was found to act as low efficacy partial agonist (Table 2).

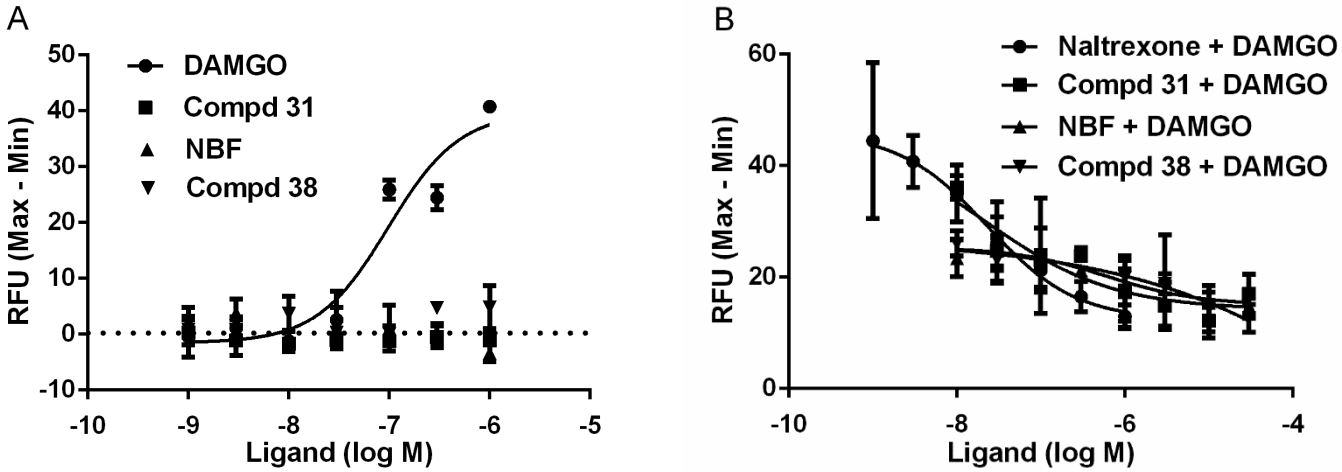

Figure 6. The calcium flux assay of compound **31**, NBF, and compound **38** in $G\alpha_{qi5}$ transfected mMOR-CHO cells. (A) Compound **31**, NBF, and compound **38** exhibited no apparent agonism to increase intracellular calcium level. DAMGO was used as a control. The assay was repeated at least three times. The EC_{50} value of DAMGO was 97.34 ± 1.35 nM. (B) Compound **31**, NBF, and compound **38** significantly antagonized DAMGO-induced intracellular calcium increase. Naltrexone was used as a control. DAMGO in assay buffer (500 nM) was used in this antagonism studies. The assay was repeated at least three times and the data is shown as the mean ± SEM. The IC_{50} values of naltrexone, compound **31**, NBF, and compound **38** were 15.37 ± 1.92 nM, 50.7 ± 2.88 nM, 566.14 ± 7.68 nM and 15.59 ± 1.96 nM, respectively.

Inhibition of cAMP Synthesis Assay. Cyclic adenosine monophosphate (cAMP) is a critical second messenger in GPCR signal transduction, which is acutely inhibited after opioid agonist couples to G_i/G_o

classes of the G-proteins.[68] We, therefore, evaluated the inhibitory effect of selected compounds on forskolin-stimulated cAMP formation compared to DAMGO in mMOR-CHO cells. Figure 7 shows that all tested ligands caused lower acute inhibition of cAMP production compared to DAMGO. As expected, the MOR full agonist DAMGO was a potent inhibitor of forskolin-stimulated cAMP formation (E_{max} = 82.4 ± 1.7%, EC_{50} = 19 ± 5 nM). Compound **31** showed an E_{max} value of 18.9 ± 3.7% inhibition at an EC_{50} value of 80 ± 21 nM, while NBF produced somewhat greater inhibition, with an E_{max} value of 35.7 ± 2.2% and an EC_{50} value of 37 ± 10 nM. On the other hand, compound **38** acted as an MOR neutral antagonist because it did not produce concentration-dependent inhibition of cAMP production at concentrations that bind to the MOR (Table 2). These results basically corresponded well with the results in [^{35}S]-GTPγS functional assays, in which the order of decreasing relative efficacy was DAMGO >> NBF > compound **31** ≈ compound **38**.

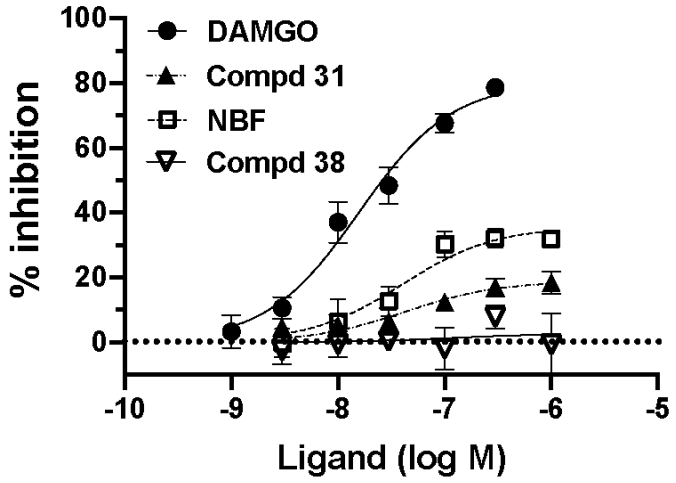

Figure 7. The inhibition of cAMP synthesis assay of NBF and compounds **31** and **38** (n = 3). NBF, compounds **31** and **38** displayed varying degree of inhibition of 10 μM forskolin-stimulated cAMP. Data are presented as mean % inhibition values ± SEM of the percentage of cAMP inhibition, where stimulation by 10 μM forskolin alone is designated as 0%.

In Vivo Opioid-Withdrawal Studies. It has been reported that the well-known opioid antagonists such as naltrexone and naloxone may precipitate significant withdrawal symptoms when administered to opioid dependent patients.[69,70] Since NBF and compounds **31** and **38** showed potent antagonisms in vivo, it is necessary to examine whether they would produce withdrawal effects in morphine-pelleted mice. Thus somatic symptoms of opioid withdrawal (wet-dog shakes, escape jumps, and paw tremors) were monitored and recorded over a 20 min period after each injection with tested compound.[71] As shown in Figure 8, naloxone precipitated significant withdrawal symptoms at 1 mg/kg (Figure 8, the second columns), which were similar to previous reports.[41,72] Meanwhile, a 20 mg/kg dose of NBF did not show any significant withdrawal signs

in placebo-pelleted mice (Figure 8, the first columns). A 1 mg/kg dose of NBF produced significantly fewer wet-dog shakes, escape jumps, and paw tremors than 1 mg/kg NLX (Figure 8A, 8B and 8C,) in morphine-pelleted mice. Moreover, the number of wet-dog shakes, escape jumps, and paw tremors for NBF at high dose of 50 mg/kg were still dramatically lower than that of 1 mg/kg naloxone. On the other hand, a 1 mg/kg dose of compound **31** produced wet-dog shakes, escape jumps, and paw tremors similar to naloxone at 1 mg/kg (Figure S4). For compound **38**, it produced significantly fewer escape jumps and slightly fewer wet-dog shakes and paw tremors at 1 mg/kg than naloxone at 1 mg/kg (Figure S5). More interestingly, at a dose of 8 mg/kg compound **38** still produced significantly fewer paw tremors (Figure S5C) than naloxone at 1 mg/kg. Overall, these results suggest NBF produced much less significant withdrawal effects than NLX, which may indicate its potential application in opioid abuse and addiction treatment.

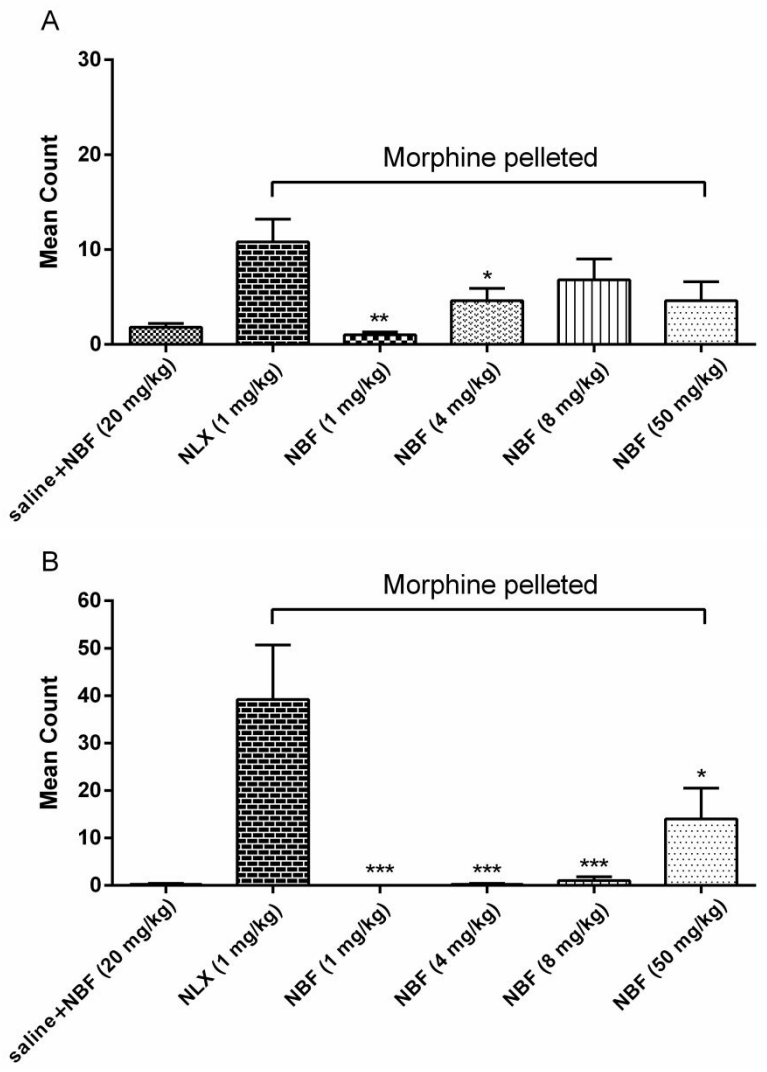

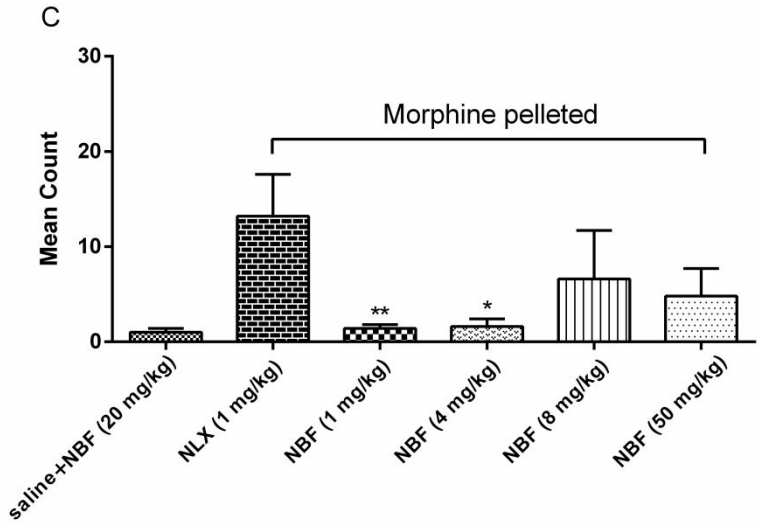

Figure 8. In vivo withdrawal assays of NBF in morphine-pelleted mice (n = 5). (A) Wet-dog shakes, (B) escape jumps, and (C) paw tremors. The first column in each figure represents placebo-pelleted mice, while the second to the fifth columns represent morphine-pelleted mice. ∗ indicates $P < 0.05$, ∗∗ indicates $P < 0.005$, ∗∗∗ indicates $P < 0.0005$, compared to 1 mg/kg naloxone (NLX, s.c.).

Conclusions

Bivalent bioisosteres represented by -NH-, -O- and -S- moieties have been widely used in drug design and lead optimization for decades. Our previous studies revealed that NAN acted as a potent MOR antagonist while its structurally similar analogue INTA actually produced agonism both in vitro and in vivo. On the basis of these observations, we thus applied the concept of "bivalent bioisostere" for the structural modification of INTA and NAN by replacing the -NH- in their indole ring with a -O- or -S- moiety. Twenty-four opioid ligands carrying benzofuran and benzothiophene moieties were prepared and pharmacologically evaluated. The competitive radioligand binding assays indicated that introduction of oxygen or sulfur atom resulted in retention of binding affinity at the MOR but somewhat changed selectivity on the MOR over the KOR or/and DOR. The [^{35}S]-GTPγS functional assay demonstrated various effects on MOR efficacy in 6β-configuration analogues and distinct reduction on MOR efficacy in 6α-configuration analogues. Molecular modeling studies revealed that NAN and INTA as well as their corresponding bioisosteric counterparts, compounds **15**, **16**, **37**, and **38** seemed bind to the MOR in similar fashions. It also suggested that compounds **15**, **16**, **37**, and **38** may act as bitopic allosteric modulators at the MOR similar to INTA and NAN. Meanwhile, similar interactions between INTA, compounds **15** and **16** and the MOR, KOR, and DOR resulted in their low selectivity to the MOR over the KOR and DOR. However, differentiated interactions between the "address" portions of NAN, compounds **37** and **38** with the allosteric binding site of the MOR, KOR, and DOR may cause NAN, compounds **37** and **38** exhibiting moderate selectivity to the MOR over the KOR and DOR. Further in vivo studies showed that three new compounds were more potent than NAN in blocking antinociceptic effect of

morphine. Particularly, compound **25** (NBF) bearing 7′-benzofuryl moiety exhibited 12-fold antagonist potency in comparison to NAN. Further investigation on the MOR-activated downstream signaling indicated that NBF, compounds **31** and **38** significantly antagonized DAMGO-induced intracellular calcium flux and exhibited varying degree of inhibition against cAMP production. Among these three potent antagonists, NBF showed much less significant withdrawal symptoms than naloxone in morphine-pelleted mice, suggesting its potential application to treat OUD. Taken together, these data demonstrated that our application of the "bivalent bioisostere concept" for structural modification of opioid ligands INTA and NAN implemented several new members of potent antagonists for the opioid receptors as well as a potential lead to develop novel therapeutic agents treating OUD.

Experimental Section.

Chemistry. All nonaqueous reactions were carried out under a pre-dried nitrogen gas atmosphere. All solvents and reagents were purchased from either Sigma-Aldrich or Alfa Aesar, and were used as received without further purification. Melting points were measured on a MPA100 OptiMelt automated melting point apparatus without correction. IR spectra were recorded on Thermo Scientific Nicolet iS10 FT-IR Spectrometer. Analytical thin-layer chromatography (TLC) analyses were carried out on Analtech Uniplate F254 plates and flash column chromatography (FCC) was performed over silica gel (230−400 mesh, Merck). ^{1}H (400 MHz) and ^{13}C (100 MHz) nuclear magnetic resonance (NMR) spectra were recorded on a Bruker Ultrashield 400 Plus spectrometer, and chemical shifts were expressed in ppm. Mass spectra were obtained on an Applied BioSystems 3200 Q trap with a turbo V source for TurbolonSpray. Analytical reversed-phase high performance liquid chromatography (HPLC) was performed on a Varian ProStar 210 system using Agilent Microsorb-MV 100-5 C18 column (250 x 4.6 mm). All analyses were conducted at ambient temperature with a flow rate of 0.8 mL/min. Mobile phase is acetonitrile/water (90/10) with 0.1% trifluoroacetic acid (TFA). The UV detector was set up at 210 nm. Compounds purities were calculated as the percentage peak area of the analyzed compound, and retention times (R_t) were presented in minutes. The purity of all newly synthesized compounds was identified as ≥ 95%.

General Procedure for Amide Coupling/Hydrolysis Reaction. A solution of carboxylic acid (2.5 equiv) in dry DMF (1.5 mL) was added with hydrobenzotriazole (HOBt, 3 equiv), *N*-(3-dimethylaminopropyl)-*N*′-ethylcarbodiimide hydrochloride (EDCI, 3 equiv), 4 Å molecular sieves, and triethylamine (5 equiv) on an ice-water bath. After 1h, a solution of 6*α*-naltrexamine or 6*β*-naltrexamine (1 equiv) in pre-dried DMF (1.5 mL) was added dropwise. The resulting mixture was stirred at room temperature. Once TLC indicated complete consumption of the starting material, the reaction mixture was filtered through celite. The filtrate was concentrated to dryness, and dissolved in anhydrous methanol (3 mL), then K_2CO_3 (2.5 equiv) was added.

The resulting mixture was stirred overnight at room temperature and filtered again over celite. After concentration, the residue was purified by flash column chromatography with CH_2Cl_2/MeOH (1% $NH_3 \cdot H_2O$) as the eluent to give the free base. After structural confirmation by ^{1}H NMR, the corresponding free base was then converted into a hydrochloride salt, which was fully characterized by ^{1}H NMR, ^{13}C NMR, IR, MS, and HPLC.

17-Cyclopropylmethyl-3,14*β*-dihydroxy-4,5*α*-epoxy-6*β*-(benzofuran-2-carboxamido)morphinan (15)

The title compound was prepared following the general procedure as a white solid in 36% yield. Hydrochloride salt: ^{1}H NMR (400 MHz, DMSO-d_6) δ 9.36 (s, 1H, exchangeable), 9.01 (d, J = 8.3 Hz, 1H, exchangeable), 8.90 (s, 1H, exchangeable), 7.79 (d, J = 7.6 Hz, 1H), 7.67 (d, J = 8.4 Hz, 1H), 7.59 (s, 1H), 7.49 (t, J = 7.5 Hz, 1H), 7.35 (t, J = 7.5 Hz, 1H), 6.74 (d, J = 8.1 Hz, 1H), 6.66 (d, J = 8.1 Hz, 1H), 6.25 (s, 1H, exchangeable), 4.90 (d, J = 7.8 Hz, 1H), 3.90 (d, J = 5.1 Hz, 1H), 3.69 (m, 1H), 3.37 (m, 1H), 3.30 (m, 1H), 3.08 (m, 1H), 3.03 (m, 1H), 2.88 (m, 1H), 2.46–2.44 (m, 2H), 1.96 (m, 1H), 1.80 (m, 1H), 1.58 (m, 1H), 1.46 (m, 1H), 1.40 (m, 1H), 1.09 (m, 1H), 0.68 (m, 1H), 0.60 (m, 1H), 0.52 (m, 1H), 0.42 (m, 1H). ^{13}C NMR (100 MHz, DMSO-d_6) δ 157.76, 154.19, 149.02, 142.09, 141.35, 129.63, 127.11, 126.83, 123.69, 122.78, 120.60, 119.31, 117.92, 111.73, 109.47, 89.62, 69.68, 61.67, 56.67, 55.00, 50.82, 45.60, 29.40, 27.31, 23.69, 23.02, 5.72, 5.10, 2.62. $[\alpha]^{25}_D$ –201.7^o (c 0.2, MeOH). HRMS calcd for $C_{29}H_{31}N_2O_5$ m/z: 487.2227. Found $[M + H]^+$ (m/z): 487.2262. IR (diamond, cm^{-1}) ν_{max} : 3064, 1652, 1597, 1448, 1313, 1177, 1028, 746. Mp 199–201 ^{o}C, dec.

17-Cyclopropylmethyl-3,14*β*-dihydroxy-4,5*α*-epoxy-6*β*-(benzothiophene-2-carboxamido)morphinan (16)

The title compound was prepared following the general procedure as a white solid in 52% yield. Hydrochloride salt: ^{1}H NMR (400 MHz, DMSO-d_6) δ 9.34 (s, 1H, exchangeable), 8.99 (d, J = 8.2 Hz, 1H, exchangeable), 8.84 (s, 1H, exchangeable), 8.15 (s, 1H), 8.03 (d, J = 7.6 Hz, 1H), 7.97 (d, J = 7.6 Hz, 1H), 7.50–7.43 (m, 2H), 6.73 (d, J = 8.1 Hz, 1H), 6.67 (d, J = 8.1 Hz, 1H), 6.13 (s, 1H, exchangeable), 4.81 (d, J = 7.8 Hz, 1H), 4.08 (m, 1H), 3.85 (d, J = 5.3 Hz, 1H), 3.66 (m, 1H), 3.37 (m, 1H), 3.26 (m, 1H), 3.10 (m, 1H), 3.05 (m, 1H), 2.85 (m, 1H), 2.43 (m, 1H), 1.91 (m, 1H), 1.76 (m, 1H), 1.63 (m, 1H), 1.50 (m, 1H), 1.43 (m, 1H), 1.07 (m, 1H), 0.68 (m, 1H), 0.60 (m, 1H), 0.51 (m, 1H), 0.42 (m, 1H). ^{13}C NMR (100 MHz, DMSO-d_6) δ 161.05, 142.09, 141.35, 140.21, 140.01, 139.14, 129.58, 126.19, 125.18, 124.89, 124.76, 122.79, 120.59, 119.36, 117.95, 89.73, 69.69, 61.72, 56.72, 51.38, 46.49, 45.62, 29.34, 27.32, 23.76, 23.03, 5.71, 5.09, 2.63. $[\alpha]^{25}_D$ –172.0^o (c 0.2, MeOH). HRMS calcd for $C_{29}H_{31}N_2O_4S$ m/z: 503.1999. Found $[M + H]^+$ (m/z): 503.1991. IR (diamond, cm^{-1}) ν_{max} : 3061, 1647, 1538, 1451, 1319, 1126, 1018, 759. Mp 273–275 ^{o}C, dec.

17-Cyclopropylmethyl-3,14*β*-dihydroxy-4,5*α*-epoxy-6*β*-(benzofuran-3-carboxamido)morphinan (17)

The title compound was prepared following the general procedure as a white solid in 49% yield. Hydrochloride salt: ^{1}H NMR (400 MHz, DMSO-d_6) δ 9.36 (s, 1H, exchangeable), 8.87 (s, 1H, exchangeable), 8.63 (s, 1H),

8.61 (d, J = 8.2 Hz, 1H, exchangeable), 8.07 (d, J = 7.3 Hz, 1H), 7.66 (d, J = 8.1 Hz, 1H), 7.40 (t, J = 7.5 Hz, 1H), 7.35 (t, J = 7.5 Hz, 1H), 6.74 (d, J = 8.1 Hz, 1H), 6.67 (d, J = 8.1 Hz, 1H), 6.18 (s, 1H, exchangeable), 4.77 (d, J = 7.8 Hz, 1H), 3.87 (d, J = 4.9 Hz, 1H), 3.71 (m, 1H), 3.38 (m, 1H), 3.35 (m, 1H), 3.10 (m, 1H), 3.05 (m, 1H), 2.86 (m, 1H), 2.46–2.44 (m, 2H), 1.90 (m, 1H), 1.78 (m, 1H), 1.65 (m, 1H), 1.49 (m, 1H), 1.41 (m, 1H), 1.08 (m, 1H), 0.69 (m, 1H), 0.60 (m, 1H), 0.51 (m, 1H), 0.43 (m, 1H). ^{13}C NMR (100 MHz, DMSO-d_6) δ 161.62, 158.15, 154.62, 147.38, 142.12, 141.32, 129.60, 125.08, 123.69, 121.93, 120.57, 119.29, 117.93, 116.85, 111.51, 89.90, 69.70, 61.72, 56.69, 54.85, 50.58, 45.61, 29.35, 27.32, 23.84, 22.59, 5.68, 5.07, 2.59. $[\alpha]^{25}_{D}$ –147.3° (c 0.2, MeOH). HRMS calcd for $C_{29}H_{31}N_2O_5$ m/z: 487.2227. Found $[M + H]^+$ (m/z): 487.2190. IR (diamond, cm^{-1}) ν_{max} : 3181, 1648, 1536, 1447, 1314, 1124, 1038, 755. Mp 241–243 °C, dec.

17-Cyclopropylmethyl-3,14*β*-dihydroxy-4,5*α*-epoxy-6*β*-(benzothiophene-3-carboxamido)morphinan (18)

The title compound was prepared following the general procedure as a white solid in 43% yield. Hydrochloride salt: ^{1}H NMR (400 MHz, DMSO-d_6) δ 9.34 (s, 1H, exchangeable), 8.84 (s, 1H, exchangeable), 8.68 (d, J = 7.9 Hz, 1H, exchangeable), 8.46 (d, J = 7.2 Hz, 1H), 8.43 (s, 1H), 8.05 (d, J = 7.2 Hz, 1H), 7.46–7.40 (m, 2H), 6.73 (d, J = 8.1 Hz, 1H), 6.67 (d, J = 8.1 Hz, 1H), 6.13 (s, 1H, exchangeable), 4.80 (d, J = 7.7 Hz, 1H), 3.85 (d, J = 5.6 Hz, 1H), 3.71 (m, 1H), 3.36 (m, 1H), 3.28 (m, 1H), 3.15 (m, 1H), 3.09–3.02 (m, 2H), 2.85 (m, 1H), 2.42 (m, 1H), 1.90 (m, 1H), 1.77 (m, 1H), 1.67 (m, 1H), 1.49 (m, 1H), 1.43 (m, 1H), 1.07 (m, 1H), 0.68 (m, 1H), 0.59 (m, 1H), 0.50 (m, 1H), 0.42 (m, 1H). ^{13}C NMR (100 MHz, DMSO-d_6) δ 162.67, 142.18, 141.35, 139.44, 137.18, 130.75, 130.72, 129.68, 124.84, 124.76, 124.58, 122.71, 120.60, 119.30, 117.95, 89.88, 69.75, 61.74, 56.72, 50.79, 46.51, 45.65, 29.43, 27.35, 23.79, 23.04, 5.72, 5.11, 2.62. $[\alpha]^{25}_{D}$ –129.0° (c 0.1, MeOH). HRMS calcd for $C_{29}H_{31}N_2O_4S$ m/z: 503.1999. Found $[M + H]^+$ (m/z): 503.1980. IR (diamond, cm^{-1}) ν_{max} : 2981, 1656, 1507, 1450, 1325, 1127, 1034, 765. Mp 254–256 °C, dec.

17-Cyclopropylmethyl-3,14*β*-dihydroxy-4,5*α*-epoxy-6*β*-(benzofuran-4-carboxamido)morphinan (19)

The title compound was prepared following the general procedure as a white solid in 42% yield. Hydrochloride salt: ^{1}H NMR (400 MHz, DMSO-d_6) δ 9.33 (s, 1H, exchangeable), 8.84 (s, 1H, exchangeable), 8.70 (d, J = 8.0 Hz, 1H, exchangeable), 8.09 (d, J = 2.1 Hz, 1H), 7.79 (d, J = 8.0 Hz, 1H), 7.77 (d, J = 7.9 Hz, 1H), 7.42 (t, J = 7.9 Hz, 1H), 7.31 (d, J = 2.1 Hz, 1H), 6.73 (d, J = 8.1 Hz, 1H), 6.67 (d, J = 8.1 Hz, 1H), 6.13 (s, 1H, exchangeable), 4.86 (d, J = 7.9 Hz, 1H), 3.86 (d, J = 5.1 Hz, 1H), 3.73 (m, 1H), 3.37 (m, 1H), 3.28 (m, 1H), 3.10 (m, 1H), 3.04 (m, 1H), 2.85 (m, 1H), 2.46–2.44 (m, 2H), 1.91 (m, 1H), 1.77 (m, 1H), 1.65 (m, 1H), 1.49 (m, 1H), 1.42 (m, 1H), 1.06 (m, 1H), 0.68 (m, 1H), 0.60 (m, 1H), 0.50 (m, 1H), 0.42 (m, 1H). ^{13}C NMR (100 MHz, DMSO-d_6) δ 165.77, 154.72, 146.90, 142.21, 141.32, 129.69, 127.60, 126.39, 123.72, 121.73, 120.58, 119.24, 117.93, 114.01, 107.31, 89.88, 69.76, 61.74, 54.87, 51.10, 46.50, 45.63, 29.45, 27.35, 23.76, 23.04, 5.71, 5.09, 2.63. $[\alpha]^{25}_{D}$ –138.4° (c 0.2, MeOH). HRMS calcd for $C_{29}H_{31}N_2O_5$ m/z: 487.2227. Found $[M + H]^+$

(m/z): 487.2206. IR (diamond, cm^{-1}) ν_{max} : 3182, 1646, 1505, 1447, 1313, 1124, 1032, 754. Mp 239–241 °C, dec.

17-Cyclopropylmethyl-3,14*β*-dihydroxy-4,5*α*-epoxy-6*β*-(benzothiophene-4-carboxamido)morphinan (20)

The title compound was prepared following the general procedure as a white solid in 53% yield. Hydrochloride salt: ^{1}H NMR (400 MHz, DMSO-d_6) δ 9.36 (s, 1H, exchangeable), 8.89 (s, 1H, exchangeable), 8.72 (d, J = 8.1 Hz, 1H, exchangeable), 8.17 (d, J = 8.1 Hz, 1H), 7.90–7.85 (m, 2H), 7.72 (d, J = 7.7 Hz, 1H), 7.46 (t, J = 7.7 Hz, 1H), 6.75 (d, J = 8.1 Hz, 1H), 6.67 (d, J = 8.1 Hz, 1H), 6.23 (s, 1H, exchangeable), 4.83 (d, J = 7.8 Hz, 1H), 3.90 (d, J = 5.3 Hz, 1H), 3.74 (m, 1H), 3.36 (m, 1H), 3.29 (m, 1H), 3.10 (m, 1H), 3.04 (m, 1H), 2.88 (m, 1H), 2.47–2.42 (m, 2H), 1.93 (m, 1H), 1.80 (m, 1H), 1.68 (m, 1H), 1.47 (m, 1H), 1.47 (m, 1H), 1.09 (m, 1H), 0.68 (m, 1H), 0.60 (m, 1H), 0.52 (m, 1H), 0.42 (m, 1H). ^{13}C NMR (100 MHz, DMSO-d_6) δ 166.98, 142.21, 141.33, 140.27, 137.15, 130.60, 129.68, 128.44, 125.02, 123.72, 123.54, 123.46, 120.57, 119.22, 117.93, 89.85, 69.73, 61.69, 56.68, 51.17, 46.47, 45.61, 29.44, 27.32, 23.68, 23.02, 5.69, 5.06, 2.59. $[\alpha]^{25}_D$ –194.0° (c 0.05, MeOH). HRMS calcd for $C_{29}H_{31}N_2O_4S$ m/z: 503.1999. Found $[M + H]^+$ (m/z): 503.1953. IR (diamond, cm^{-1}) ν_{max} : 2973, 1655, 1505, 1323, 1298, 1126, 1034, 765. Mp 250 °C, dec.

17-Cyclopropylmethyl-3,14*β*-dihydroxy-4,5*α*-epoxy-6*β*-(benzofuran-5-carboxamido)morphinan (21)

The title compound was prepared following the general procedure as a white solid in 40% yield. Hydrochloride salt: ^{1}H NMR (400 MHz, DMSO-d_6) δ 9.33 (s, 1H, exchangeable), 8.86 (s, 1H, exchangeable), 8.70 (d, J = 8.0 Hz, 1H, exchangeable), 8.24 (d, J = 1.7 Hz, 1H), 8.09 (d, J = 2.2 Hz, 1H), 7.88 (dd, J = 8.7, 1.7 Hz, 1H), 7.68 (d, J = 8.7 Hz, 1H), 7.08 (d, J = 2.2 Hz, 1H), 6.73 (d, J = 8.1 Hz, 1H), 6.66 (d, J = 8.1 Hz, 1H), 6.15 (s, 1H, exchangeable), 4.86 (d, J = 7.8 Hz, 1H), 3.86 (d, J = 5.1 Hz, 1H), 3.71 (m, 1H), 3.37 (m, 1H), 3.34 (m, 1H), 3.10 (m, 1H), 3.04 (m, 1H), 2.85 (m, 1H), 2.47–2.44 (m, 2H), 1.89 (m, 1H), 1.77 (m, 1H), 1.62 (m, 1H), 1.48 (m, 1H), 1.41 (m, 1H), 1.07 (m, 1H), 0.68 (m, 1H), 0.59 (m, 1H), 0.51 (m, 1H), 0.42 (m, 1H). ^{13}C NMR (100 MHz, DMSO-d_6) δ 165.70, 155.76, 147.19, 142.20, 141.31, 129.69, 129.45, 127.02, 123.86, 120.88, 120.58, 119.23, 117.92, 110.91, 107.16, 89.91, 69.75, 61.75, 54.87, 51.26, 46.50, 45.61, 29.39, 27.37, 23.80, 23.04, 5.71, 5.09, 2.63. $[\alpha]^{25}_D$ –162.1° (c 0.2, MeOH). HRMS calcd for $C_{29}H_{31}N_2O_5$ m/z: 487.2227. Found $[M + H]^+$ (m/z): 487.2230. IR (diamond, cm^{-1}) ν_{max} : 3098, 1644, 1503, 1464, 1311, 1253, 1124, 748. Mp 298–300 °C, dec.

17-Cyclopropylmethyl-3,14*β*-dihydroxy-4,5*α*-epoxy-6*β*-(benzothiophene-5-carboxamido)morphinan (22)

The title compound was prepared following the general procedure as a white solid in 55% yield. Hydrochloride salt: ^{1}H NMR (400 MHz, DMSO-d_6) δ 9.34 (s, 1H, exchangeable), 8.88 (s, 1H, exchangeable), 8.77 (d, J = 8.1 Hz, 1H, exchangeable), 8.45 (s, 1H), 8.11 (d, J = 8.1 Hz, 1H), 7.88 (d, J = 8.1 Hz, 1H), 7.87 (d, J = 5.2

Hz, 1H), 7.56 (d, J = 5.2 Hz, 1H), 6.73 (d, J = 8.1 Hz, 1H), 6.66 (d, J = 8.1 Hz, 1H), 6.21 (s, 1H, exchangeable), 4.88 (d, J = 7.8 Hz, 1H), 3.88 (d, J = 5.1 Hz, 1H), 3.74 (m, 1H), 3.37 (m, 1H), 3.27 (m, 1H), 3.09 (m, 1H), 3.04 (m, 1H), 2.87 (m, 1H), 2.48–2.44 (m, 2H), 1.91 (m, 1H), 1.78 (m, 1H), 1.63 (m, 1H), 1.48 (m, 1H), 1.41 (m, 1H), 1.09 (m, 1H), 0.68 (m, 1H), 0.60 (m, 1H), 0.51 (m, 1H), 0.42 (m, 1H). ^{13}C NMR (100 MHz, DMSO-d_6) δ 165.77, 142.19, 141.74, 141.31, 139.15, 130.67, 129.68, 128.76, 124.38, 122.89, 122.78, 122.38, 120.58, 119.25, 117.92, 89.91, 69.75, 61.76, 56.70, 51.27, 46.50, 45.61, 29.38, 27.37, 23.79, 23.04, 5.71, 5.09, 2.62. $[\alpha]^{25}_{D}$ –130.6° (c 0.05, MeOH). HRMS calcd for $C_{29}H_{31}N_2O_4S$ m/z: 503.1999. Found $[M + H]^+$ (m/z): 503.1923. IR (diamond, cm^{-1}) ν_{max} : 3096, 1646, 1501, 1424, 1309, 1128, 1032, 748. Mp 289–291 °C, dec.

17-Cyclopropylmethyl-3,14*β*-dihydroxy-4,5*α*-epoxy-6*β*-(benzofuran-6-carboxamido)morphinan (23)

The title compound was prepared following the general procedure as a white solid in 44% yield. Hydrochloride salt: ^{1}H NMR (400 MHz, DMSO-d_6) δ 9.34 (s, 1H, exchangeable), 8.85 (s, 1H, exchangeable), 8.72 (d, J = 7.9 Hz, 1H, exchangeable), 8.16 (d, J = 2.1 Hz, 1H), 8.15 (s, 1H), 7.84 (dd, J = 8.2, 1.3 Hz, 1H), 7.75 (d, J = 8.2 Hz, 1H), 7.05 (d, J = 2.1 Hz, 1H), 6.73 (d, J = 8.1 Hz, 1H), 6.67 (d, J = 8.1 Hz, 1H), 6.13 (s, 1H，exchangeable), 4.86 (d, J = 7.8 Hz, 1H), 3.85 (d, J = 5.3 Hz, 1H), 3.72 (m, 1H), 3.37 (m, 1H), 3.29 (m, 1H), 3.09 (m, 1H), 3.04 (m, 1H), 2.84 (m, 1H), 2.47–2.42 (m, 2H), 1.89 (m, 1H), 1.76 (m, 1H), 1.63 (m, 1H), 1.49 (m, 1H), 1.41 (m, 1H), 1.08 (m, 1H), 0.69 (m, 1H), 0.60 (m, 1H), 0.50 (m, 1H), 0.42 (m, 1H). ^{13}C NMR (100 MHz, DMSO-d_6) δ 165.44, 153.93, 148.34, 142.19, 141.31, 130.54, 129.88, 129.68, 122.17, 120.87, 120.59, 119.25, 117.92, 110.22, 106.82, 89.88, 69.75, 61.74, 56.71, 51.31, 46.50, 45.61, 29.38, 27.35, 23.79, 23.02, 5.71, 5.06, 2.63. $[\alpha]^{25}_{D}$ –147.4° (c 0.2, MeOH). HRMS calcd for $C_{29}H_{31}N_2O_5$ m/z: 487.2227. Found $[M + H]^+$ (m/z): 487.2238. IR (diamond, cm^{-1}) ν_{max} : 3102, 1637, 1527, 1448, 1312, 1126, 1032, 747. Mp 283–284 °C, dec.

17-Cyclopropylmethyl-3,14*β*-dihydroxy-4,5*α*-epoxy-6*β*-(benzothiophene-6-carboxamido)morphinan (24)

The title compound was prepared following the general procedure as a white solid in 47% yield. Hydrochloride salt: ^{1}H NMR (400 MHz, DMSO-d_6) δ 9.34 (s, 1H, exchangeable), 8.89 (s, 1H, exchangeable), 8.78 (d, J = 8.0 Hz, 1H, exchangeable), 8.56 (s, 1H), 7.97 (d, J = 8.4 Hz, 1H), 7.95 (d, J = 5.4 Hz, 1H), 7.91 (d, J = 8.4 Hz, 1H), 7.54 (d, J = 5.4 Hz, 1H), 6.74 (d, J = 8.1 Hz, 1H), 6.66 (d, J = 8.1 Hz, 1H), 6.23 (s, 1H, exchangeable), 4.87 (d, J = 7.8 Hz, 1H), 3.89 (d, J = 5.1 Hz, 1H), 3.73 (m, 1H), 3.37 (m, 1H), 3.32 (m, 1H), 3.09 (m, 1H), 3.05 (m, 1H), 2.87 (m, 1H), 2.47–2.44 (m, 2H), 1.92 (m, 1H), 1.79 (m, 1H), 1.63 (m, 1H), 1.48 (m, 1H), 1.41 (m, 1H), 1.09 (m, 1H), 0.68 (m, 1H), 0.60 (m, 1H), 0.52 (m, 1H), 0.42 (m, 1H). ^{13}C NMR (100 MHz, DMSO-d_6) δ 165.50, 142.16, 141.40, 141.29, 138.85, 130.40, 130.21, 129.65, 123.83, 123.27, 123.25, 121.85, 120.56, 119.23, 117.90, 89.89, 69.72, 61.71, 56.68, 51.28, 46.47, 45.58, 29.34, 27.33, 23.75, 23.01, 5.68, 5.06, 2.59. $[\alpha]^{25}_{D}$ –142.0° (c 0.1, MeOH). HRMS calcd for $C_{29}H_{31}N_2O_4S$ m/z: 503.1999. Found $[M + H]^+$ (m/z): 503.1989.

IR (diamond, cm^{-1}) ν_{max} : 3095, 1645, 1502, 1425, 1310, 1187, 1032, 748. Mp 266–267 °C, dec.

17-Cyclopropylmethyl-3,14*β*-dihydroxy-4,5*α*-epoxy-6*β*-(benzofuran-7-carboxamido)morphinan (25)

The title compound was prepared following the general procedure as a white solid in 45% yield. Hydrochloride salt: ^{1}H NMR (400 MHz, DMSO-d_6) δ 9.37 (s, 1H, exchangeable), 8.91 (s, 1H, exchangeable), 8.47 (d, J = 8.3 Hz, 1H, exchangeable), 8.14 (d, J = 2.1 Hz, 1H), 7.84 (dd, J = 7.7, 1.0 Hz, 1H), 7.71 (d, J = 7.7 Hz, 1H), 7.36 (t, J = 7.7 Hz, 1H), 7.09 (d, J = 2.1 Hz, 1H), 6.75 (d, J = 8.1 Hz, 1H), 6.66 (d, J = 8.1 Hz, 1H), 6.35 (s, 1H, exchangeable), 4.91 (d, J = 7.7 Hz, 1H), 3.91 (d, J = 5.0 Hz, 1H), 3.79 (m, 1H), 3.34 (m, 1H), 3.30 (m, 1H), 3.09 (m, 1H), 3.04 (m, 1H), 2.88 (m, 1H), 2.47–2.43 (m, 2H), 1.99 (m, 1H), 1.79 (m, 1H), 1.65 (m, 1H), 1.46 (m, 1H), 1.39 (m, 1H), 1.09 (m, 1H), 0.68 (m, 1H), 0.60 (m, 1H), 0.52 (m, 1H), 0.42 (m, 1H). ^{13}C NMR (100 MHz, DMSO-d_6) δ 163.35, 151.01, 146.36, 142.19, 141.29, 129.66, 128.23, 124.54, 124.40, 122.79, 120.59, 119.24, 119.10, 117.91, 106.86, 90.01, 69.72, 61.58, 56.68, 51.18, 46.47, 45.66, 29.45, 27.32, 23.66, 22.98, 5.68, 5.06, 2.59. $[\alpha]^{25}_D$ –99.8° (c 0.2, MeOH). HRMS calcd for $C_{29}H_{31}N_2O_5$ m/z: 487.2227. Found [M + H]$^+$ (m/z): 487.2190. IR (diamond, cm^{-1}) ν_{max} : 3064, 1644, 1505, 1451, 1316, 1125, 1032, 749. Mp 270–272 °C, dec.

17-Cyclopropylmethyl-3,14*β*-dihydroxy-4,5*α*-epoxy-6*β*-(benzothiophene-7-carboxamido)morphinan (26)

The title compound was prepared following the general procedure as a white solid in 55% yield. Hydrochloride salt: ^{1}H NMR (400 MHz, DMSO-d_6) δ 9.34 (s, 1H, exchangeable), 8.96 (d, J = 8.0 Hz, 1H, exchangeable), 8.88 (s, 1H, exchangeable), 8.10 (d, J = 7.7 Hz, 1H), 8.07 (d, J = 7.7 Hz, 1H), 7.81 (d, J = 5.6 Hz, 1H), 7.53 (t, J = 7.7 Hz, 1H), 7.49 (d, J = 5.6 Hz, 1H), 6.74 (d, J = 8.1 Hz, 1H), 6.68 (d, J = 8.1 Hz, 1H), 6.22 (s, 1H, exchangeable), 4.91 (d, J = 7.8 Hz, 1H), 3.89 (d, J = 5.2 Hz, 1H), 3.76 (m, 1H), 3.37 (m, 1H), 3.29 (m, 1H), 3.10 (m, 1H), 3.05 (m, 1H), 2.87 (m, 1H), 2.47–2.42 (m, 2H), 1.94 (m, 1H), 1.80 (m, 1H), 1.65 (m, 1H), 1.49 (m, 1H), 1.42 (m, 1H), 1.09 (m, 1H), 0.69 (m, 1H), 0.60 (m, 1H), 0.51 (m, 1H), 0.43 (m, 1H). ^{13}C NMR (100 MHz, DMSO-d_6) δ 165.30, 142.14, 141.30, 140.82, 138.11, 130.88, 129.62, 127.32, 126.79, 123.84, 122.86, 122.52, 120.55, 119.26, 117.94, 89.71, 69.73, 61.73, 56.69, 51.34, 46.47, 45.62, 29.40, 27.33, 23.73, 23.02, 5.68, 5.05, 2.60. $[\alpha]^{25}_D$ –114.0° (c 0.1, MeOH). HRMS calcd for $C_{29}H_{31}N_2O_4S$ m/z: 503.1999. Found [M + H]$^+$ (m/z): 503.1984. IR (diamond, cm^{-1}) ν_{max} : 3096, 1647, 1502, 1425, 1312, 1128, 1033, 748. Mp 259–261 °C, dec.

17-Cyclopropylmethyl-3,14*β*-dihydroxy-4,5*α*-epoxy-6*α*-(benzofuran-2-carboxamido)morphinan (27)

The title compound was prepared following the general procedure as a white solid in 56% yield. Hydrochloride salt: ^{1}H NMR (400 MHz, DMSO-d_6) δ 9.26 (s, 1H, exchangeable), 8.85 (s, 1H, exchangeable), 8.13 (d, J = 7.9 Hz, 1H, exchangeable), 7.79 (d, J = 7.6 Hz, 1H), 7.70 (d, J = 8.4 Hz, 1H), 7.65 (s, 1H), 7.49 (t, J = 7.6 Hz, 1H), 7.35 (t, J = 7.6 Hz, 1H), 6.74 (d, J = 8.1 Hz, 1H), 6.60 (d, J = 8.1 Hz, 1H), 6.32 (s, 1H, exchangeable),

4.79 (d, J = 3.8 Hz, 1H), 4.63 (m, 1H), 3.92 (d, J = 6.7 Hz, 1H), 3.34 (m, 1H), 3.27 (m, 1H), 3.09 (m, 1H), 3.05 (m, 1H), 2.96 (m, 1H), 2.73 (m, 1H), 2.47 (m, 1H), 1.92 (m, 1H), 1.65 (m, 1H), 1.56 (m, 1H), 1.47 (m, 1H), 1.17 (m, 1H), 1.07 (m, 1H), 0.70 (m, 1H), 0.62 (m, 1H), 0.48 (m, 1H), 0.41 (m, 1H). ^{13}C NMR (100 MHz, DMSO-d_6) δ 157.61, 154.23, 148.71, 145.92, 138.87, 128.65, 127.10, 126.92, 123.75, 122.77, 122.07, 119.27, 118.37, 111.85, 109.99, 87.09, 69.34, 64.86, 61.02, 57.04, 45.61, 45.29, 30.18, 29.15, 23.48, 19.44, 5.68, 5.15, 2.56. $[\alpha]^{25}_{D}$ –227.3° (c 0.25, MeOH). HRMS calcd for $C_{29}H_{31}N_2O_5$ m/z: 487.2227. Found $[M + H]^+$ (m/z): 487. 2233. IR (diamond, cm^{-1}) ν_{max}: 3061, 1645, 1505, 1449, 1316, 1117, 1032, 749. Mp 244–246 °C, dec.

17-Cyclopropylmethyl-3,14*β*-dihydroxy-4,5*α*-epoxy-6*α*-(benzothiophene-2-carboxamido)morphinan (28)

The title compound was prepared following the general procedure as a white solid in 43% yield. Hydrochloride salt: ^{1}H NMR (400 MHz, DMSO-d_6) δ 9.24 (s, 1H, exchangeable), 8.86 (s, 1H, exchangeable), 8.48 (d, J = 7.5 Hz, 1H, exchangeable), 8.28 (s, 1H), 8.03 (d, J = 7.1 Hz, 1H), 7.95 (d, J = 7.1 Hz, 1H), 7.49–7.45 (m, 2H), 6.73 (d, J = 8.1 Hz, 1H), 6.59 (d, J = 8.1 Hz, 1H), 6.34 (s, 1H, exchangeable), 4.79 (d, J = 3.8 Hz, 1H), 4.60 (m, 1H), 3.93 (d, J = 6.7 Hz, 1H), 3.39 (m, 1H), 3.27 (m, 1H), 3.08 (m, 1H), 3.04 (m, 1H), 2.96 (m, 1H), 2.73 (m, 1H), 2.47 (m, 1H), 1.93 (m, 1H), 1.65 (m, 1H), 1.54 (m, 1H), 1.46 (m, 1H), 1.22 (m, 1H), 1.07 (m, 1H), 0.69 (m, 1H), 0.62 (m, 1H), 0.49 (m, 1H), 0.41 (m, 1H). ^{13}C NMR (100 MHz, DMSO-d_6) δ 161.13, 146.05, 140.19, 139.63, 139.14, 138.80, 128.63, 126.19, 125.37, 125.13, 124.90, 122.75, 122.04, 119.12, 118.31, 86.97, 69.35, 61.04, 57.01, 51.97, 46.25, 45.23, 30.24, 29.17, 23.46, 19.17, 5.65, 5.13, 2.54. $[\alpha]^{25}_{D}$ –197.7° (c 0.2, MeOH). HRMS calcd for $C_{29}H_{31}N_2O_4S$ m/z: 503.1999. Found $[M + H]^+$ (m/z): 503.1952. IR (diamond, cm^{-1}) ν_{max} : 2942, 1621, 1505, 1455, 1303, 1117, 1032, 755. Mp 240–242 °C, dec.

17-Cyclopropylmethyl-3,14*β*-dihydroxy-4,5*α*-epoxy-6*α*-(benzofuran-3-carboxamido)morphinan (29)

The title compound was prepared following the general procedure as a white solid in 60% yield. Hydrochloride salt: ^{1}H NMR (400 MHz, DMSO-d_6) δ 9.23 (s, 1H, exchangeable), 8.87 (s, 1H, exchangeable), 8.74 (s, 1H), 8.11 (d, J = 7.8 Hz, 1H, exchangeable), 8.08 (dd, J = 7.2, 1.1 Hz, 1H), 7.66 (dd, J = 7.2, 1.1 Hz, 1H), 7.41–7.35 (m, 2H), 6.72 (d, J = 8.1 Hz, 1H), 6.58 (d, J = 8.1 Hz, 1H), 6.34 (s, 1H, exchangeable), 4.80 (d, J = 3.9 Hz, 1H), 4.64 (m, 1H), 3.94 (d, J = 6.8 Hz, 1H), 3.37 (m, 1H), 3.28 (m, 1H), 3.08 (m, 1H), 3.04 (m, 1H), 2.96 (m, 1H), 2.73 (m, 1H), 2.53 (m, 1H), 1.93 (m, 1H), 1.65 (m, 1H), 1.54 (m, 1H), 1.46 (m, 1H), 1.16 (m, 1H), 1.09 (m, 1H), 0.69 (m, 1H), 0.62 (m, 1H), 0.49 (m, 1H), 0.41 (m, 1H). ^{13}C NMR (100 MHz, DMSO-d_6) δ 161.61, 154.54, 147.83, 146.07, 138.80, 128.69, 125.26, 125.03, 123.73, 122.05, 121.80, 119.09, 118.34, 116.58, 111.53, 87.19, 69.36, 61.06, 57.01, 45.42, 45.21, 30.22, 29.20, 23.47, 19.39, 5.65, 5.12, 2.54. $[\alpha]^{25}_{D}$ – 145.0° (c 0.2, MeOH). HRMS calcd for $C_{29}H_{31}N_2O_5$ m/z: 487.2227. Found $[M + H]^+$ (m/z): 487.2225. IR (diamond, cm^{-1}) ν_{max} : 2973, 1646, 1505, 1451, 1316, 1117, 1031, 748. Mp 229–231 °C, dec.

17-Cyclopropylmethyl-3,14*β*-dihydroxy-4,5*α*-epoxy-6*α*-(benzothiophene-3-carboxamido)morphinan (30)

The title compound was prepared following the general procedure as a white solid in 33% yield. Hydrochloride salt: ^{1}H NMR (400 MHz, DMSO-d_6) δ 9.19 (s, 1H, exchangeable), 8.89 (s, 1H, exchangeable), 8.47 (s, 1H), 8.45 (dd, J = 7.2, 1.5 Hz, 1H), 8.17 (d, J = 7.7 Hz, 1H, exchangeable), 8.06 (dd, J = 7.2, 1.5 Hz, 1H), 7.49 (t, J = 7.2 Hz, 1H), 7.43 (t, J = 7.2 Hz, 1H), 6.72 (d, J = 8.1 Hz, 1H), 6.58 (d, J = 8.1 Hz, 1H), 6.35 (s, 1H, exchangeable), 4.83 (d, J = 3.9 Hz, 1H), 4.64 (m, 1H), 3.95 (d, J = 6.8 Hz, 1H), 3.38 (m, 1H), 3.28 (m, 1H), 3.09 (m, 1H), 3.05 (m, 1H), 2.97 (m, 1H), 2.74 (m, 1H), 2.54 (m, 1H), 1.94 (m, 1H), 1.67 (m, 1H), 1.56 (m, 1H), 1.47 (m, 1H), 1.18 (m, 1H), 1.08 (m, 1H), 0.70 (m, 1H), 0.62 (m, 1H), 0.49 (m, 1H), 0.42 (m, 1H). ^{13}C NMR (100 MHz, DMSO-d_6) δ 162.68, 146.06, 139.35, 138.80, 137.17, 131.05, 130.82, 128.71, 124.82, 124.77, 124.34, 122.74, 122.07, 119.09, 118.30, 87.13, 69.36, 61.06, 57.02, 56.09, 45.62, 45.22, 30.21, 29.23, 23.47, 19.40, 5.66, 5.13, 2.54. $[\alpha]^{25}_D$ –233.2° (c 0.2, MeOH). HRMS calcd for $C_{29}H_{31}N_2O_4S$ m/z: 503.1999. Found $[M + H]^+$ (m/z): 503.1935. IR (diamond, cm^{-1}) ν_{max} : 2942, 1621, 1505, 1455, 1303, 1117, 1032, 755. Mp 225 °C, dec.

17-Cyclopropylmethyl-3,14*β*-dihydroxy-4,5*α*-epoxy-6*α*-(benzofuran-4-carboxamido)morphinan (31)

The title compound was prepared following the general procedure as a white solid in 45% yield. Hydrochloride salt: ^{1}H NMR (400 MHz, DMSO-d_6) δ 9.17 (s, 1H, exchangeable), 8.88 (s, 1H, exchangeable), 8.10 (d, J = 2.2 Hz, 1H), 8.09 (d, J = 7.2 Hz, 1H, exchangeable), 7.79 (d, J = 8.2 Hz, 1H), 7.72 (d, J = 7.2 Hz, 1H), 7.41 (t, J = 7.9 Hz, 1H), 7.31 (dd, J = 2.2, 0.8 Hz, 1H), 6.72 (d, J = 8.1 Hz, 1H), 6.58 (d, J = 8.1 Hz, 1H), 6.33 (s, 1H, exchangeable), 4.84 (d, J = 3.8 Hz, 1H), 4.64 (m, 1H), 3.94 (d, J = 6.7 Hz, 1H), 3.38 (m, 1H), 3.27 (m, 1H), 3.09 (m, 1H), 3.06 (m, 1H), 2.97 (m, 1H), 2.74 (m, 1H), 2.54 (m, 1H), 1.94 (m, 1H), 1.67 (m, 1H), 1.55 (m, 1H), 1.47 (m, 1H), 1.17 (m, 1H), 1.09 (m, 1H), 0.70 (m, 1H), 0.63 (m, 1H), 0.49 (m, 1H), 0.41 (m, 1H). ^{13}C NMR (100 MHz, DMSO-d_6) δ 165.93, 154.61, 146.93, 146.06, 138.85, 128.75, 127.98, 126.21, 123.74, 122.21, 122.10, 119.14, 118.31, 113.93, 107.05, 87.19, 69.36, 61.08, 57.06, 51.39, 45.88, 45.24, 30.21, 29.29, 24.84, 19.45, 5.67, 5.15, 2.56. $[\alpha]^{25}_D$ –257.0° (c 0.2, MeOH). HRMS calcd for $C_{29}H_{31}N_2O_5$ m/z: 487.2227. Found $[M + H]^+$ (m/z): 487.2236. IR (diamond, cm^{-1}) ν_{max} : 2972, 1645, 1505, 1449, 1316, 1118, 1032, 748. Mp 224–226 °C, dec.

17-Cyclopropylmethyl-3,14*β*-dihydroxy-4,5*α*-epoxy-6*α*-(benzothiophene-4-carboxamido)morphinan (32)

The title compound was prepared following the general procedure as a white solid in 41% yield. Hydrochloride salt: ^{1}H NMR (400 MHz, DMSO-d_6) δ 8.21 (d, J = 7.7 Hz, 1H, exchangeable), 8.15 (d, J = 8.1 Hz, 1H), 7.87–7.82 (m, 2H), 7.67 (d, J = 7.7 Hz, 1H), 7.44 (t, J = 7.7 Hz, 1H), 6.70 (d, J = 8.1 Hz, 1H), 6.59 (d, J = 8.1 Hz, 1H), 4.84 (d, J = 3.8 Hz, 1H), 4.62 (m, 1H), 3.91 (d, J = 6.9 Hz, 1H), 3.29 (m, 1H), 3.25 (m, 1H), 3.09 (m,

1H), 3.04 (m, 1H), 2.94 (m, 1H), 2.74 (m, 1H), 2.53 (m, 1H), 1.90 (m, 1H), 1.66 (m, 1H), 1.55 (m, 1H), 1.45 (m, 1H), 1.13 (m, 1H), 1.04 (m, 1H), 0.70 (m, 1H), 0.62 (m, 1H), 0.47 (m, 1H), 0.40 (m, 1H). ^{13}C NMR (100 MHz, DMSO-d_6) δ 167.08, 146.04, 140.11, 138.83, 137.08, 130.92, 128.73, 128.48, 124.89, 123.82, 123.57, 123.55, 122.08, 119.09, 118.26, 87.10, 69.34, 61.05, 57.02, 45.90, 45.22, 30.18, 29.25, 23.48, 19.43, 5.65, 5.12, 2.54. $[\alpha]^{25}_{D}$ –182.5° (*c* 0.2, MeOH). HRMS calcd for $C_{29}H_{31}N_2O_4S$ m/z: 503.1999. Found $[M + H]^+$ (m/z): 503.1940. IR (diamond, cm^{-1}) ν_{max} : 2956, 1622, 1504, 1455, 1303, 1117, 1031, 769. Mp 242–243 °C, dec.

17-Cyclopropylmethyl-3,14*β*-dihydroxy-4,5*α*-epoxy-6*α*-(benzofuran-5-carboxamido)morphinan (33)

The title compound was prepared following the general procedure as a white solid in 51% yield. Hydrochloride salt: ^{1}H NMR (400 MHz, DMSO-d_6) δ 9.18 (s, 1H, exchangeable), 8.86 (s, 1H, exchangeable), 8.23 (d, J = 1.5 Hz, 1H), 8.10 (d, J = 2.2 Hz, 1H), 8.09 (d, J = 8.1 Hz, 1H, exchangeable), 7.87 (dd, J = 8.6, 1.5 Hz, 1H), 7.69 (d, J = 8.6 Hz, 1H), 7.08 (d, J = 2.2 Hz, 1H), 6.72 (d, J = 8.1 Hz, 1H), 6.58 (d, J = 8.1 Hz, 1H), 6.31 (s, 1H, exchangeable), 4.80 (d, J = 3.9 Hz, 1H), 4.62 (m, 1H), 3.93 (d, J = 6.8 Hz, 1H), 3.38 (m, 1H), 3.27 (m, 1H), 3.08 (m, 1H), 3.05 (m, 1H), 2.96 (m, 1H), 2.73 (m, 1H), 2.53 (m, 1H), 1.92 (m, 1H), 1.65 (m, 1H), 1.53 (m, 1H), 1.46 (m, 1H), 1.18 (m, 1H), 1.07 (m, 1H), 0.69 (m, 1H), 0.62 (m, 1H), 0.49 (m, 1H), 0.41 (m, 1H). ^{13}C NMR (100 MHz, DMSO-d_6) δ 166.07, 155.74, 147.19, 146.07, 138.79, 129.62, 128.72, 126.92, 124.16, 122.07, 121.08, 119.06, 118.30, 110.88, 107.13, 87.22, 69.38, 61.03, 57.00, 46.02, 45.20, 30.21, 29.23, 23.50, 19.40, 5.67, 5.14, 2.55. $[\alpha]^{25}_{D}$ –183.1° (*c* 0.25, MeOH). HRMS calcd for $C_{29}H_{31}N_2O_5$ m/z: 487.2227. Found $[M + H]^+$ (m/z): 487. 2308. IR (diamond, cm^{-1}) ν_{max} : 2972, 1624, 1505, 1452, 1317, 1237, 1115, 1031, 746. Mp 257–258 °C, dec.

17-Cyclopropylmethyl-3,14*β*-dihydroxy-4,5*α*-epoxy-6*α*-(benzothiophene-5-carboxamido)morphinan (34)

The title compound was prepared following the general procedure as a white solid in 36% yield. Hydrochloride salt: ^{1}H NMR (400 MHz, DMSO-d_6) δ 9.20 (s, 1H, exchangeable), 8.88 (s, 1H, exchangeable), 8.44 (s, 1H), 8.16 (d, J = 7.6 Hz, 1H, exchangeable), 8.11 (d, J = 8.4 Hz, 1H), 7.89–7.85 (m, 2H), 7.57 (d, J = 7.6 Hz, 1H), 6.73 (d, J = 8.1 Hz, 1H), 6.58 (d, J = 8.1 Hz, 1H), 6.36 (s, 1H, exchangeable), 4.81 (d, J = 3.8 Hz, 1H), 4.64 (m, 1H), 3.95 (d, J = 6.7 Hz, 1H), 3.37 (m, 1H), 3.26 (m, 1H), 3.08 (m, 1H), 3.05 (m, 1H), 2.97 (m, 1H), 2.73 (m, 1H), 2.53 (m, 1H), 1.94 (m, 1H), 1.65 (m, 1H), 1.54 (m, 1H), 1.46 (m, 1H), 1.21 (m, 1H), 1.09 (m, 1H), 0.69 (m, 1H), 0.62 (m, 1H), 0.49 (m, 1H), 0.41 (m, 1H). ^{13}C NMR (100 MHz, DMSO-d_6) δ 166.15, 146.04, 141.72, 139.04, 138.79, 130.81, 128.73, 128.71, 124.34, 123.22, 122.94, 122.33, 122.05, 119.08, 118.29, 87.19, 69.37, 61.06, 57.01, 46.03, 45.21, 30.21, 29.21, 23.48, 19.40, 5.66, 5.13, 2.54. $[\alpha]^{25}_{D}$ –156.1° (*c* 0.1, MeOH). HRMS calcd for $C_{29}H_{31}N_2O_4S$ m/z: 503.1999. Found $[M + H]^+$ (m/z): 503.1934. IR (diamond, cm^{-1}) ν_{max} : 2942, 1620, 1560, 1454, 1320, 1116, 1073, 730. Mp 256–258 °C, dec.

17-Cyclopropylmethyl-3,14*β*-dihydroxy-4,5*α*-epoxy-6*α*-(benzofuran-6-carboxamido)morphinan (35)

The title compound was prepared following the general procedure as a white solid in 62% yield. Hydrochloride salt: ^{1}H NMR (400 MHz, DMSO-d_6) δ 9.17 (s, 1H, exchangeable), 8.84 (s, 1H, exchangeable), 8.15 (d, J = 2.2 Hz, 1H), 8.14 (d, J = 8.0 Hz, 1H, exchangeable), 8.12 (s, 1H), 7.82 (d, J = 8.1 Hz, 1H), 7.75 (d, J = 8.1 Hz, 1H), 7.05 (d, J = 2.2 Hz, 1H), 6.71 (d, J = 8.1 Hz, 1H), 6.58 (d, J = 8.1 Hz, 1H), 6.29 (s, 1H, exchangeable), 4.80 (d, J = 3.9 Hz, 1H), 4.63 (m, 1H), 3.91 (d, J = 6.8 Hz, 1H), 3.36 (m, 1H), 3.26 (m, 1H), 3.08 (m, 1H), 3.05 (m, 1H), 2.95 (m, 1H), 2.73 (m, 1H), 2.47 (m, 1H), 1.92 (m, 1H), 1.65 (m, 1H), 1.54 (m, 1H), 1.47 (m, 1H), 1.20 (m, 1H), 1.07 (m, 1H), 0.70 (m, 1H), 0.62 (m, 1H), 0.49 (m, 1H), 0.41 (m, 1H). ^{13}C NMR (100 MHz, DMSO-d_6) δ 165.80, 153.79, 148.29, 146.05, 138.78, 130.66, 129.83, 128.70, 122.43, 122.03, 120.81, 119.05, 118.26, 110.53, 106.80, 87.14, 69.36, 64.83, 61.06, 57.01, 46.07, 45.19, 30.21, 29.20, 23.47, 19.32, 5.65, 5.12, 2.53. $[\alpha]^{25}_D$ –167.0° (c 0.2, MeOH). HRMS calcd for $C_{29}H_{31}N_2O_5$ m/z: 487.2227. Found $[M + H]^+$ (m/z): 487.2310. IR (diamond, cm^{-1}) ν_{max} : 2973, 1644, 1505, 1451, 1316, 1117, 1032, 746. Mp 250–252 °C, dec.

17-Cyclopropylmethyl-3,14*β*-dihydroxy-4,5*α*-epoxy-6*α*-(benzothiophene-6-carboxamido)morphinan (36)

The title compound was prepared following the general procedure as a white solid in 48% yield. Hydrochloride salt: ^{1}H NMR (400 MHz, DMSO-d_6) δ 9.18 (s, 1H, exchangeable), 8.85 (s, 1H, exchangeable), 8.55 (s, 1H), 8.16 (d, J = 7.6 Hz, 1H, exchangeable), 7.98 (d, J = 8.3 Hz, 1H), 7.96 (d, J = 5.5 Hz, 1H), 7.89 (d, J = 8.3 Hz, 1H), 7.55 (d, J = 5.5 Hz, 1H), 6.72 (d, J = 8.1 Hz, 1H), 6.59 (d, J = 8.1 Hz, 1H), 6.29 (s, 1H, exchangeable), 4.81 (d, J = 3.8 Hz, 1H), 4.63 (m, 1H), 3.92 (d, J = 6.6 Hz, 1H), 3.36 (m, 1H), 3.26 (m, 1H), 3.08 (m, 1H), 3.05 (m, 1H), 2.96 (m, 1H), 2.73 (m, 1H), 2.47 (m, 1H), 1.92 (m, 1H), 1.66 (m, 1H), 1.55 (m, 1H), 1.47 (m, 1H), 1.20 (m, 1H), 1.08 (m, 1H), 0.70 (m, 1H), 0.62 (m, 1H), 0.49 (m, 1H), 0.41 (m, 1H). ^{13}C NMR (100 MHz, DMSO-d_6) δ 165.82, 153.82, 148.33, 146.07, 138.81, 130.68, 129.86, 128.72, 122.46, 122.06, 120.83, 119.08, 118.28, 110.56, 106.83, 87.16, 69.39, 64.86, 61.07, 57.02, 46.09, 45.21, 30.25, 29.23, 23.50, 19.35, 5.68, 5.15, 2.56. $[\alpha]^{25}_D$ –254.0° (c 0.1, MeOH). HRMS calcd for $C_{29}H_{31}N_2O_4S$ m/z: 503.1999. Found $[M + H]^+$ (m/z): 503.1918. IR (diamond, cm^{-1}) ν_{max} : 2971, 1634, 1506, 1456, 1317, 1117, 774. Mp 258 °C, dec.

17-Cyclopropylmethyl-3,14*β*-dihydroxy-4,5*α*-epoxy-6*α*-(benzofuran-7-carboxamido)morphinan (37)

The title compound was prepared following the general procedure as a white solid in 49% yield. Hydrochloride salt: ^{1}H NMR (400 MHz, DMSO-d_6) δ 9.25 (s, 1H, exchangeable), 8.86 (s, 1H, exchangeable), 8.07 (d, J = 2.2 Hz, 1H), 8.04 (d, J = 8.1 Hz, 1H, exchangeable), 7.88 (dd, J = 7.7, 1.1 Hz, 1H), 7.81 (dd, J = 7.7, 1.1 Hz, 1H), 7.39 (t, J = 7.7 Hz, 1H), 7.12 (d, J = 2.2 Hz, 1H), 6.72 (d, J = 8.1 Hz, 1H), 6.61 (d, J = 8.1 Hz, 1H), 6.32 (s, 1H, exchangeable), 4.84 (d, J = 3.9 Hz, 1H), 4.70 (m, 1H), 3.93 (d, J = 6.6 Hz, 1H), 3.37 (m, 1H), 3.25 (m, 1H), 3.11 (m, 1H), 3.05 (m, 1H), 2.95 (m, 1H), 2.73 (m, 1H), 2.54 (m, 1H), 1.93 (m, 1H), 1.73–1.64 (m, 2H),

1.49 (m, 1H), 1.07 (m, 1H), 0.99 (m, 1H), 0.70 (m, 1H), 0.62 (m, 1H), 0.49 (m, 1H), 0.41 (m, 1H). ^{13}C NMR (100 MHz, DMSO-d_6) δ 162.69, 151.05, 146.28, 145.64, 139.04, 128.84, 128.15, 124.98, 124.89, 123.05, 122.03, 119.42, 118.33, 118.26, 107.08, 87.24, 69.29, 64.86, 61.04, 57.05, 45.64, 45.27, 30.00, 29.20, 23.48, 20.28, 5.68, 5.13, 2.59. $[\alpha]^{25}_{D}$ –168.5° (*c* 0.2, MeOH). HRMS calcd for $C_{29}H_{31}N_2O_5$ m/z: 487.2227. Found $[M + H]^+$ (m/z): 487.2327. IR (diamond, cm^{-1}) ν_{max} : 2973, 1646, 1506, 1451, 1316, 1117, 1032, 748. Mp 257–259 °C, dec.

17-Cyclopropylmethyl-3,14*β*-dihydroxy-4,5*α*-epoxy-6*α*-(benzothiophene-7-carboxamido)morphinan (38)

The title compound was prepared following the general procedure as a white solid in 32% yield. Hydrochloride salt: ^{1}H NMR (400 MHz, DMSO-d_6) δ 9.21 (s, 1H, exchangeable), 8.88 (s, 1H, exchangeable), 8.35 (d, J = 7.5 Hz, 1H, exchangeable), 8.10 (d, J = 7.7 Hz, 1H), 8.08 (d, J = 7.7 Hz, 1H), 7.83 (d, J = 5.5 Hz, 1H), 7.53 (t, J = 7.7 Hz, 1H), 7.51 (d, J = 5.5 Hz, 1H), 6.72 (d, J = 8.1 Hz, 1H), 6.59 (d, J = 8.1 Hz, 1H), 6.34 (s, 1H, exchangeable), 4.84 (d, J = 3.8 Hz, 1H), 4.67 (m, 1H), 3.94 (d, J = 6.8 Hz, 1H), 3.37(m, 1H), 3.27 (m, 1H), 3.09 (m, 1H), 3.06 (m, 1H), 2.97 (m, 1H), 2.74 (m, 1H), 2.55 (m, 1H), 1.94 (m, 1H), 1.67 (m, 1H), 1.55 (m, 1H), 1.48 (m, 1H), 1.24 (m, 1H), 1.09 (m, 1H), 0.70 (m, 1H), 0.62 (m, 1H), 0.50 (m, 1H), 0.42 (m, 1H). ^{13}C NMR (100 MHz, DMSO-d_6) δ 165.47, 146.04, 140.72, 138.79, 138.09, 130.62, 128.66, 127.42, 126.80, 123.80, 123.26, 123.01, 122.04, 119.10, 118.27, 87.02, 69.35, 64.84, 61.05, 57.02, 46.18, 45.26, 30.24, 29.27, 23.47, 19.30, 5.65, 5.13, 2.53. $[\alpha]^{25}_{D}$ –228.0° (*c* 0.05, MeOH). HRMS calcd for $C_{29}H_{31}N_2O_4S$ m/z: 503.1999. Found $[M + H]^+$ (m/z): 503.1930. IR (diamond, cm^{-1}) ν_{max} : 2971, 1621, 1504, 1455, 1318, 1116, 1031, 747. Mp 264 °C, dec.

Biological Evaluation. Drugs. Morphine (morphine sulfate pentahydrate salt) was purchased from Mallinckrodt (St. Louis, MO) or provided by the National Institute of Drug Abuse (NIDA). Naltrexone was purchased from Sigma-Aldrich (St. Louis, MO). All drugs and test compounds were dissolved in pyrogen-free isotonic saline (Baxter Healthcare, Deerfield, IL) or sterile-filtered distilled/deionized water. All other reagents and radioligands were purchased from either Sigma-Aldrich or Thermo Fisher.

Animals. **Animals.** Male Swiss Webster mice (25−30 g, 7−8 weeks, Harlan Laboratories, Indianapolis, IN) were housed in a temperature-controlled (20-22°C) AAALAC-accredited facility in which they had *ad libitum* access to food and water. The mice were maintained on a 12 h/12 h light-dark cycle (0600-1800 lights on) for the duration of the experiment and were tested during the light segment of this cycle. Mice arrived at the

vivarium housed 4/cage, and following one-week habituation were separated into individual cages. Mice were allowed to acclimate to individual caging for at least 24 h and then were randomly assigned to the various treatment conditions before the start of studies. Experimenters were blinded to these treatment conditions during the duration of the experiment and data analysis. No adverse events occurred during the experiment and no mice were excluded from data analysis. Protocols and procedures (Animal Welfare Assurance Number D16-00180) were approved by the Institutional Animal Care and Use Committee (IACUC) at Virginia Commonwealth University Medical Center and complied with the recommendations of the IASP (International Association for the Study of Pain).

In Vitro Competitive Radioligand Binding Assay. The competition binding assay was conducted using monoclonal mice opioid receptor expressed in Chinese hamster ovary (CHO) cell lines (monoclonal human δ opioid receptor was used in the DOR assay). In this assay, 30 μg of membrane protein was incubated with the corresponding radioligand in the presence of different concentrations of test compounds in TME buffer (50 mM Tris, 3 mM $MgCl_2$, and 0.2 mM EGTA, pH 7.7) for 1.5 h at 30 °C. The bound radioligand was separated by filtration using the Brandel harvester. Specific (i.e., opioid receptor-related) binding at the MOR, KOR and DOR was determined as the difference in binding obtained in the absence and presence of 5 μM naltrexone, U50,488 and SNC80, respectively. The IC_{50} values were determined and converted to K_i values using the Cheng–Prusoff equation.[73]

In Vitro [^{35}S]-GTPγS Functional Assay. In the [^{35}S]-GTPγS functional assay, 10 μg of MOR-CHO membrane protein was incubated with 10 μM GDP, 0.1 nM [^{35}S]-GTPγS and varying concentrations of the compound under investigation for 1.5 h in a 30 °C water bath. The Bradford protein assay was utilized to determine and adjust the concentration of protein required for the assay. Non-specific binding was determined with 20 μM unlabeled GTPγS. TME buffer (50 mM Tris-HCl, 3 mM $MgCl_2$, 0.2 mM EGTA, pH 7.4) with 100 mM NaCl was used to increase agonist stimulated binding and the final volume in each assay tube was 500 μl. Furthermore, 3 μM of DAMGO was included in the assay as maximally effective concentration of a full agonist for the MOR. After the incubation, the

bound radioactive ligand was separated from the free radioligand by filtration through a GF/B glass fiber filter paper and rinsed three times with ice-cold wash buffer (50 mM Tris-HCl, pH 7.2) using the Brandel harvester. The results were determined by utilizing a scintillation counter. All assays were determined in triplicate and repeated at least three times. Percent DAMGO-stimulated [^{35}S]-GTPγS binding was defined as (net-stimulated binding by ligand/net-stimulated binding by 3 μM DAMGO) x 100%.

Data Analysis of [^{35}S]-GTPγS Binding and Functional Assay. The assays of all samples were conducted in duplicate and repeated at least four times for a total of ≥4 independent determinations. Results were reported as mean values ± SEM. Concentration−effect curves were fit by nonlinear regression to a one-site binding model, using GraphPad Prism software, to determine EC_{50} and E_{max} values. IC_{50} values were obtained from Hill plots, analyzed by linear regression using GraphPad Prism software. By using the Cheng−Prusoff equation: $K_i = IC_{50}/[1 + ([L]/K_D)]$, where [L] is the concentration of competitor and K_D is the K_D of the radioligand, binding K_i values were determined from IC_{50} values. The E_{max} values for receptors were calculated as relative to net full agonist-stimulated [^{35}S]-GTPγS binding, which is defined as (net-stimulated binding by ligand/net-stimulated binding by maximally effective concentration of a full agonist) × 100%. By using the equation K_e = [Ant]/DR-1, where [Ant] is the concentration of antagonist and DR is the ratio of the DAMGO EC_{50} of values in the presence and absence of antagonist, K_e values in the competitive antagonism studies were determined.

Molecular Modeling Study. The crystal structures of antagonist-bound MOR, KOR, and DOR (PDB ID: 4DKL, 4DJH, and 4EJ4)[59,62,63] and agonist-bound MOR and KOR (PDB ID: 5C1M and 6B73)[58,64] were downloaded from Protein Data Bank at http://www.rcsb.org. Before docking, hydrogen atoms were firstly added to both receptors by Sybyl-X 2.0 (TRIPOS Inc., St. Louis, MO). INTA, NAN, compounds **15**, **16**, **37**, and **38** were also sketched in Sybyl-X 2.0. Each compound was energy minimized to a gradient of 0.05 with Gasteiger-Hückel charges assigned under the Tripos force field (TFF). Docking program GOLD 5.6 was applied to conduct the studies.[57] The atoms within 10 Å of the γ-carbon atom of ASP147 in both crystal structures were used to define the binding site. The distance constraint of 4 Å between the piperidine quaternary ammonium nitrogen atom of the compounds' epoxymorphinan nucleus and ASP147, and the hydrogen bond between the compounds' dihydrofuran oxygen atom and the phenolic oxygen atom of TYR148

were set up during the automated docking processes. In addition, from our previous study, the stable binding modes of INTA with agonist-bound MOR and NAN with antagonist-bound MOR after 10 ns molecular dynamics (MD) simulations have been obtained. Taking the fitness scores, the binding modes of INTA and NAN in the MOR, and the binding orientation of each compound within the binding site of the receptor into considerations, the highest scored solutions were selected and merged into the respective receptors to obtain the optimal binding poses of each compound. Each optimal binding pose was optimized by a 10,000-iterations minimization under TAFF in Sybyl-X 2.0 to remove the clashes and strain energies of receptor-ligand complex.

Warm Water Immersion Assay. Swiss-Webster mice (5 male mice for each group, 25−30 g, 7−8 weeks) were used in this assay. Antinociception for all synthesized compounds was conducted using male Swiss-Webster mice. The water bath temperature was set as 56 ± 0.1 °C. The baseline latency (control) was determined before injecting the compounds into the mice. The average baseline latency obtained for this experiment was 3.0 ± 0.1 s and only mice with a baseline latency of 2 to 4 s were used. To test for agonism, the tail immersion was done 20 min (time that morphine effect starts to peak) after injecting the test compounds. To prevent tissue damage, a 10 s maximum cut off time was imposed. Antinociceptive response was calculated as the percentage maximum possible effect (%MPE), where %MPE = [(test - control)/ (10 - control)] x 100. In the antagonism study, the test compounds were given 5 min before morphine. The tail immersion test was then conducted 20 min after giving morphine. %MPE was calculated for each mouse using at least five mice per compound. AD_{50} values were calculated using the least-squares linear regression analysis followed by calculation of 95% confidence interval by Bliss method.

Opioid-Withdrawal Studies. Swiss Webster mice (5 male mice for each group, 25−30 g, 7−8 weeks) were used for opioid-withdrawal studies. Following previously reported protocol, a 75 mg morphine pellet was implanted into the base of the neck of the mice, and the mice were allowed to recover in their home cages. Before tested, 30 min was given to the mice for habituation to an open-topped, square, clear Plexiglas observation chamber (26 × 26 × 26 cm^3) with lines partitioning the bottom into quadrants. All drugs and test compounds were administered subcutaneously (s.c.). The withdrawal was precipitated 72 h from pellet implantation with naloxone (1 mg/kg, s.c.) and the test compounds at different doses. Withdrawal commenced within 3 min after antagonist administration. Escape jumps, paw tremors, and wet dog shakes were quantified

by counting their occurrences over 20 min for each mouse (five mice per group). The data is presented as the mean ± SEM.

Calcium Flux Assay. A Chinese hamster ovary cell line stably expressing the mouse mu opioid receptor (mMOR-CHO) was used for this assay. The cells were transfected with $G\alpha_{qi5}$ for 4 hours and then plated (10,000 cells/well) to black 96-well plates with clear bottoms (Greiner Bio-One). After 24 hours of incubation, the culture media was removed and the cells were washed with assay buffer (50 mL HBSS, 1 mL HEPES, 250 μL probenecid, 50 μL 1mM $CaCl_2$, 50 μL 1mM $MgCl_2$). The hydrochloride salts of tested compounds were dissolved in DMSO as a stock solution for assay (1 M). For agonist assays, cells were then incubated with 50 μL/well loading buffer (6 mL assay buffer, 24 μL Fluo4-AM solution (Invitrogen), 12 μL probenecid solution) for 60 min. Following incubation, different concentrations of the test compound was added by FlexStation3 microplate reader (Molecular Devices) and read at ex494/em516. Each concentration was run in triplicate. For antagonism studies, the cells were incubated with the same loading buffer as the agonist assay for 60 min. Then, different concentrations of the test compound (20 μL/well) was manually added to each well followed by another 15 min incubation. After that, the solution of DAMGO in assay buffer (500 nM) or just assay buffer (blank) was added by FlexStation3 microplate reader (Molecular Devices) and read at ex494/em516. Each concentration was run in triplicate. The corresponding EC_{50} or IC_{50} value of each compound was calculated by non-linear regression using GraphPad Prism 6.0 (GraphPad Software, San Diego, CA).

Inhibition of cAMP Synthesis. The mMOR-CHO cells were grown in a 96-well plate containing DMEM/F12 media until confluency. Cells were pre-incubated for 30 minutes at 37°C with phosphodieasterase inhibitors (1 mM IBMX and 200 μM Ro 20-1724), bovine albumin serum and (20 mM, pH 7.2-7.5) HEPES prior to the addition of opioid ligands. After an 8 min incubation at 37°C with the tested ligand and 10 μM forskolin, the reaction was terminated by removing the media and rinsing with phosphate-buffered saline (kept at room temperature). DMEM/F12 media was used as a solvent for all chemicals. Forskolin (10 μM) was used to stimulate adenylyl cyclase and the inhibition of forskolin-stimulated activity was measured. The cAMP level was detected with ELISA using the commercially available cAMP direct EIA kit (K019-H5) from ARBOR ASSAYS® on a Turner Biosystems Modulus™ microplate reader.

Statistical Analysis. One-way ANOVA followed by the posthoc Dunnett test were performed to assess significance using Prism 6.0 software (GraphPad Software, San Diego, CA).

ASSOCIATED CONTENT

Supporting Information.

Molecular formula strings and some data (CSV)

Spectra data for target compounds (^{1}H NMR, ^{13}C NMR, and HPLC graphs)

Synthesis of benzo[*b*]thiophene-6-carboxylic acid

Table S1. Measured Shortest Distances between Atoms on Critical Amino Acid Residues and Atoms on the Compounds from the Docking Poses after Energy Minimization.

Figure S1. Structures of INTA (a), Compound **15** (b), Compound **16** (c), NAN (d), Compound **37** (e), and Compound **38** (f) with Atom Notation Derived from the Complexes Obtained from Docking Studies.

Figure S2. The binding modes of INTA-KOR^{active} (a), Compound 15-KOR^{active} (b), and Compound 16-KOR^{active} (c), NAN-KOR^{inactive} (d), Compound 37-KOR^{inactive} (e), and Compound 38-KOR^{inactive} (f) from molecular docking studies.

Figure S3. The binding modes of INTA-DOR^{inactive} (a), Compound 15-DOR^{inactive} (b), and Compound 16-DOR^{inactive} (c), NAN-DOR^{inactive} (d), Compound 37-DOR^{inactive} (e), and Compound 38-DOR^{inactive} (f) from molecular docking studies.

Figure S4. In vivo withdrawal study of compound **31** in morphine-pelleted mice.

Figure S5. In vivo withdrawal study of compound **38** in morphine-pelleted mice.

These material are available free of charge.

AUTHOR INFORMATION

Corresponding Author

*Phone: +1 (804) 828-0021. Fax: +1 (804) 828-7625. E-mail: yzhang2@vcu.edu.

Author Contributions

Y. Zhang conceived and oversaw the project and finalized the manuscript. H. Ma conducted the chemical synthesis. H. Ma and H. Wang drafted the manuscript. S. Obeng, A. M. Jali, and D. L. Stevens conducted radioligand binding assays and in vivo studies under the supervision of D. E. Selley and W. L. Dewey. Y.

Zheng and M. Li conducted calcium flux assay under the supervision of Y. Zhang. A. M. Jali conducted cAMP poduction assay under the supervision of D. E. Selley. H. Wang finished the docking studies under the supervision of Y. Zhang.

Notes

The authors declare no competing financial interest.

Funding Sources

This work was partially supported by NIH/NIDA Grants DA024022, DA044855 and DA050311 (Y.Z.). Naltrexone (free base) was provided through NIDA Drug Supply Program. The content is solely the responsibility of the authors and does not necessarily represent the official views of the National Institute on Drug Abuse or the National Institutes of Health.

ABBREVIATIONS USED

GPCR, G-protein-coupled receptor; MOR, μ opioid receptor; KOR, κ opioid receptor; DOR, δ opioid receptor; DAMGO, [D-Ala2-MePhe4-Gly(ol)5]enkephalin; INTA, 17-Cyclopropylmethyl-3,14β-dihydroxy-4,5α-epoxy-6β-(indole-2-carboxamido)morphinan; NAN, 17-Cyclopropylmethyl-3,14β-dihydroxy-4,5α-epoxy-6α-(indole-7-carboxamido)morphinan; cAMP, cyclic adenosine monophosphate; TFF, TRIPOS force field; CHO, Chinese hamster ovary; CL, confidence level; %MPE, percentage maximum possible effect; NIDA, National Institute of Drug Abuse

References

1. Beckett, A. H.; Casy, A. F. Synthetic analgesics: stereochemical considerations. *J. Pharm. Pharmacol.* **1954**, *6*, 986–1001.

2. Portoghese, P. S. A new concept on the mode of interaction of narcotic analgesics with receptors. *J. Med. Chem.* **1965**, *8*, 609–616.

3. Simon, E. J.; Hiller, J. M.; Edelman, I. Stereospecific binding of the potent narcotic analgesic [^{3}H] Etorphine to rat-brain homogenate. *Proc. Natl. Acad. Sci. U.S.A* **1973**, *70*, 1947–1949.

4. Pert, C. B.; Snyder, S. H. Opiate receptor: demonstration in nervous tissue. *Science* **1973**, *179*, 1011–1014.

5. Dhawan, B. N.; Cesselin, F.; Raghubir, R.; Reisine, T.; Bradley, P. B.; Portoghese, P. S.; Hamon, M. International Union of Pharmacology. XII. Classification of opioid receptors. *Pharmacol. Rev.* **1996**, *48*, 567–592.

6. Pasternak, G. W. Opioids and their receptors: Are we there yet? *Neuropharmacology* **2014**, *76*, 198–203.

7. Shang, Y.; Filizola, M. Opioid receptors: Structural and mechanistic insights into pharmacology and signaling. *Eur. J. Pharmacol.* **2015**, *763*, 206–213.

8. Xia, Y.; Haddad, G. G. Ontogeny and distribution of opioid receptors in the rat brainstem. *Brain Res.* **1991**, *549*, 181–193.

9. Xia, Y.; Haddad, G. G. Major difference in the expression of delta- and mu-opioid receptors between turtle and rat brain. *J. Comp. Neurol.* **2001**, *436*, 202–210.

10. Wittert, G.; Hope, P.; Pyle, D. Tissue distribution of opioid receptor gene expression in the rat. *Biochem. Biophys. Res. Commun.* **1996**, *218*, 877–881.

11. Komai, H.; McDowell, T. S. Effects of local anesthetics on opioid inhibition of calcium current in rat dorsal root ganglion neurons. *Neurosci. Lett.* **2007**, *418*, 298–303.

12. Rola, R.; Jarkiewicz, M.; Szulczyk, P. Modulation of Ca^{2+} channel current by mu opioid receptors in prefrontal cortex pyramidal neurons in rats. *Acta. Neurobiol Exp. (Wars)* **2008**, *68*, 10–25.

13. Iegorova, O.; Fisyunov, A.; Krishtal, O. G-protein-independent modulation of P-type calcium channels by mu-opioids in Purkinje neurons of rat. *Neurosci. Lett.* **2010**, *480*, 106–111.

14. Donahue, R. N.; McLaughlin, P. J.; Zagon, I. S. Cell proliferation of human ovarian cancer is regulated by the opioid growth factor-opioid growth factor receptor axis. *Am. J. Physiol. Regul. Integr. Comp. Physiol.* **2009**, *296*, R1716–R1725.

15. Avella, D. M.; Kimchi, E. T.; Donahue, R. N.; Tagaram, H. R.; McLaughlin, P. J.; Zagon, I. S.; Staveley-O'Carroll, K. F. The opioid growth factor-opioid growth factor receptor axis regulates cell proliferation of human hepatocellular cancer. *Am. J. Physiol. Regul. Integr. Comp. Physiol.* **2010**, *298*, R459–R466.

16. Taracha, E.; Mierzejewski, P.; Lehner, M.; Chrapusta, S. J.; Kala, M.; Lechowicz, W.; Hamed, A.; Skorzewska, A.; Kostowski, W.; Plaznik, A. Stress-opioid interactions: a comparison of morphine and methadone. *Pharmacol. Rep.* **2009**, *61*, 424–435.

17. Vien, T. N.; Gleason, C. A.; Hays, S. L.; McPherson, R. J.; Chavkin, C.; Juul, S. E. Effects of neonatal stress and morphine on kappa opioid receptor signaling. *Neonatology* **2009**, *96*, 235–243.

18. Wikstrom, B.; Gellert, R.; Ladefoged, S. D.; Danda, Y.; Akai, M.; Ide, K.; Ogasawara, M.; Kawashima, Y.; Ueno, K.; Mori, A.; Ueno, Y. Kappa-opioid system in uremic pruritus: multicenter, randomized, double-

blind, placebo-controlled clinical studies. *J. Am. Soc. Nephrol.* **2005**, *16*, 3742–3747.

19. Iselin-Chaves, I. A.; Grotzsch, H.; Besson, M.; Burkhard, P. R.; Savoldelli, G. L. Naloxone-responsive acute dystonia and parkinsonism following general anaesthesia. *Anaesthesia* **2009**, *64*, 1359–1362.

20. Zesiewicz, T. A.; Hauser, R. A.; Freeman, A.; Sullivan, K. L.; Miller, A. M.; Halim, T. Fentanyl-induced bradykinesia and rigidity after deep brain stimulation in a patient with Parkinson disease. *Clin. Neuropharmacol.* **2009**, *32*, 48–50.

21. Li, A. H.; Wang, H. L. G protein-coupled receptor kinase 2 mediates mu-opioid receptor desensitization in GABAergic neurons of the nucleus raphe magnus. *J. Neurochem.* **2001**, *77*, 435–444.

22. Matthes, H. W.; Maldonado, R.; Simonin, F.; Valverde, O.; Slowe, S.; Kitchen, I.; Befort, K.; Dierich, A.; Le Meur, M.; Dolle, P.; Tzavara, E.; Hanoune, J.; Roques, B. P.; Kieffer, B. L. Loss of morphine-induced analgesia, reward effect and withdrawal symptoms in mice lacking the mu-opioid-receptor gene. *Nature* **1996**, *383*, 819–823.

23. Roth, B. L.; Baner, K.; Westkaemper, R.; Siebert, D.; Rice, K. C.; Steinberg, S.; Ernsberger, P.; Rothman, R. B. Salvinorin A: a potent naturally occurring nonnitrogenous kappa opioid selective agonist. *Proc. Natl. Acad. Sci. U. S. A.* **2002**, *99*, 11934–11939.

24. Saitoh, A.; Yamada, M.; Yamada, M.; Takahashi, K.; Yamaguchi, K.; Murasawa, H.; Nakatani, A.; Tatsumi, Y.; Hirose, N.; Kamei, J. Antidepressant-like effects of the delta-opioid receptor agonist SNC80 ([(+)-4-[(alpha*R*)-alpha-[(2*S*,5*R*)-2,5-dimethyl-4-(2-propenyl)-1-piperazinyl]-(3-methoxyphenyl)methyl]-*N*,*N*-diethylbenzamide) in an olfactory bulbectomized rat model. *Brain Res.* **2008**, *1208*, 160–169.

25. Reinscheid, R. K.; Nothacker, H. P.; Bourson, A.; Ardati, A.; Henningsen, R. A.; Bunzow, J. R.; Grandy, D. K.; Langen, H.; Monsma, F. J., Jr.; Civelli, O. Orphanin FQ: a neuropeptide that activates an opioidlike G protein-coupled receptor. *Science* **1995**, *270*, 792–794.

26. Feng, Y.; He, X. Z.; Yang, Y. L.; Chao, D. M.; Lazarus, L. H.; Xia, Y. Current research on opioid receptor function. *Curr. Drug Targets* **2012**, *13*, 230–246.

27. Zimmerman, D. M.; Leander, J. D. Selective opioid receptor agonists and antagonists - research tools and potential therapeutic agents. *J. Med. Chem.* **1990**, *33*, 895–902.

28. Eguchi, M. Recent advances in selective opioid receptor agonists and antagonists. *Med. Res. Rev.* **2004**, *24*, 182–212.

29. Veilleux, J. C.; Colvin, P. J.; Anderson, J.; York, C.; Heinz, A. J. A review of opioid dependence treatment: pharmacological and psychosocial interventions to treat opioid addiction. *Clin. Psychol. Rev.* **2010**, *30*, 155–166.

30. Bart, G. Maintenance medication for opiate addiction: the foundation of recovery. *J. Addict. Dis.* **2012**, *31*, 207–225.

31. Rudd, R. A.; Seth, P.; David, F.; Scholl, L. Increases in Drug and Opioid-Involved Overdose Deaths-United States, 2010–2015. *MMWR Morb Mortal Wkly Rep* **2016**, *65*, 1445–1452.

32. Isbell, H.; Vogel, V. H. The addiction liability of methadone (amidone, dolophine, 10820) and its use in the treatment of the morphine abstinence syndrome. *Am. J. Psychiatry* **1949**, *105*, 909–914.

33. Walsh, S. L.; Preston, K. L.; Stitzer, M. L.; Cone, E. J.; Bigelow, G. E. Clinical pharmacology of buprenorphine: Ceiling effects at high doses. *Clin. Pharmacol. Ther.* **1994**, *55*, 569–580.

34. O'Brien, C. P.; Greenstein, R. A.; Mintz, J.; Woody, G. E. Clinical experience with naltrexone. *Am. J. Drug Alcohol Abuse* **1975**, *2*, 365–377.

35. Li, G.; Aschenbach, L. C.; He, H.; Selley, D. E.; Zhang, Y. 14-*O*-heterocyclic-substituted naltrexone derivatives as non-peptide mu opioid receptor selective antagonists: design, synthesis, and biological studies. *Bioorg. Med. Chem. Lett.* **2009**, *19*, 1825–1829.

36. Li, G.; Aschenbach, L. C.; Chen, J.; Cassidy, M. P.; Stevens, D. L.; Gabra, B. H.; Selley, D. E.; Dewey, W. L.; Westkaemper, R. B.; Zhang, Y. Design, synthesis, and biological evaluation of 6*α*- and 6*β*-*N*-heterocyclic substituted naltrexamine derivatives as mu opioid receptor selective antagonists. *J. Med. Chem.* **2009**, *52*, 1416–1427.

37. Yuan, Y.; Elbegdorj, O.; Chen, J.; Akubathini, S. K.; Beletskaya, I. O.; Selley, D. E.; Zhang, Y. Structure selectivity relationship studies of 17-cyclopropylmethyl-3,14*β*-dihydroxy-4,5*α*-epoxy-6*β*-[(4'-pyridyl)carboxamido]morphinan derivatives toward the development of the mu opioid receptor antagonists. *Bioorg. Med. Chem. Lett.* **2011**, *21*, 5625–5629.

38. Yuan, Y.; Elbegdorj, O.; Chen, J.; Akubathini, S. K.; Zhang, F.; Stevens, D. L.; Beletskaya, I. O.; Scoggins, K. L.; Zhang, Z.; Gerk, P. M.; Selley, D. E.; Akbarali, H. I.; Dewey, W. L.; Zhang, Y. Design, synthesis, and biological evaluation of 17-cyclopropylmethyl-3,14*β*-dihydroxy-4,5*α*-epoxy-6*β*-[(4'-pyridyl)carboxamido]morphinan derivatives as peripheral selective mu opioid receptor Agents. *J. Med. Chem.* **2012**, *55*, 10118–10129.

39. Yuan, Y.; Zaidi, S. A.; Stevens, D. L.; Scoggins, K. L.; Mosier, P. D.; Kellogg, G. E.; Dewey, W. L.; Selley, D. E.; Zhang, Y. Design, syntheses, and pharmacological characterization of 17-cyclopropylmethyl-3,14*β*-dihydroxy-4,5*α*-epoxy-6*α*-(isoquinoline-3'-carboxamido)morphinan analogues as opioid receptor ligands. *Bioorg. Med. Chem.* **2015**, *23*, 1701–1715.

40. Yuan, Y.; Zaidi, S. A.; Elbegdorj, O.; Aschenbach, L. C.; Li, G.; Stevens, D. L.; Scoggins, K. L.; Dewey, W. L.; Selley, D. E.; Zhang, Y. Design, synthesis, and biological evaluation of 14-heteroaromatic-substituted naltrexone derivatives: pharmacological profile switch from mu opioid receptor selectivity to mu/kappa opioid receptor dual selectivity. *J. Med. Chem.* **2013**, *56*, 9156–9169.

41. Zheng, Y.; Obeng, S.; Wang, H.; Jali, A. M.; Peddibhotla, B.; Williams, D. A.; Zou, C. C.; Stevens, D.

L.; Dewey, W. L.; Akbarali, H. I.; Selley, D. E.; Zhang, Y. Design, synthesis, and biological evaluation of the third generation 17-cyclopropylmethyl-3,14*β*-dihydroxy-4,5*α*-epoxy-6*β*-[(4'-pyridyl)carboxamido] morphinan (NAP) derivatives as *μ*/*κ* opioid receptor dual selective ligands. *J. Med. Chem.* **2019**, *62*, 561–574.

42. Obeng, S.; Wang, H.; Jali, A.; Stevens, D. L.; Akbarali, H. I.; Dewey, W. L.; Selley, D. E.; Zhang, Y. Structure-activity relationship studies of 6*α*- and 6*β*-indolylacetamidonaltrexamine derivatives as bitopic mu opioid receptor modulators and elaboration of the "message-address concept" to comprehend their functional conversion. *ACS Chem. Neurosci.* **2019**, *10*, 1075–1090.

43. Le Naour, M.; Lunzer, M. M.; Powers, M. D.; Kalyuzhny, A. E.; Benneyworth, M. A.; Thomas, M. J.; Portoghese, P. S. Putative kappa opioid heteromers as targets for developing analgesics free of adverse effects. *J. Med. Chem.* **2014**, *57*, 6383–6392.

44. Fronik, P.; Gaiser, B. I.; Sejer Pedersen, D. Bitopic ligands and metastable binding sites: opportunities for G Protein-Coupled Receptor (GPCR) medicinal chemistry. *J. Med. Chem.* **2017**, *60*, 4126–4134.

45. Mohr, K.; Schmitz, J.; Schrage, R.; Trankle, C.; Holzgrabe, U. Molecular alliance-from orthosteric and allosteric ligands to dualsteric/bitopic agonists at G protein coupled receptors. *Angew. Chem. Int. Ed. Engl.* **2013**, *52*, 508–516.

46. Remesic, M.; Hruby, V. J.; Porreca, F.; Lee, Y. S. Recent advances in the realm of allosteric modulators for opioid receptors for future therapeutics. *ACS Chem. Neurosci.* **2017**, *8*, 1147–1158.

47. Christopoulos, A. Advances in G protein-coupled receptor allostery: from function to structure. *Mol. Pharmacol.* **2014**, *86*, 463–478.

48. Friedman, H. L. Influence of isosteric replacements upon biological activity. *NASNRS* **1951**, *206*, 295–358.

49. Patani, G. A.; LaVoie, E. J. Bioisosterism: A rational approach in drug design. *Chem. Rev.* **1996**, *96*, 3147–3176.

50. Meanwell, N. A. Synopsis of some recent tactical application of bioisosteres in drug design. *J. Med. Chem.* **2011**, *54*, 2529–2591.

51. Crilly, J. The history of clozapine and its emergence in the US market: a review and analysis. *Hist. Psychiatry* **2007**, *18*, 39–60.

52. Popovic, D.; Nuss, P.; Vieta, E. Revisiting loxapine: a systematic review. *Ann. Gen. Psychiatry* **2015**, *14*.

53. Riedel, M.; Muller, N.; Strassnig, M.; Spellmann, I.; Severus, E.; Moller, H. J. Quetiapine in the treatment of schizophrenia and related disorders. *Neuropsychiatr. Dis. Treat.* **2007**, *3*, 219–235.

54. Forest, M. C.; Lahouratate, P.; Martin, M.; Nadler, G.; Quiniou, M. J.; Zimmermann, R. G. A novel class of cardiotonic agents: synthesis and biological evaluation of 5-substituted 3,6-dihydrothiadiazin-2-ones with cyclic AMP phosphodiesterase inhibiting and myofibrillar calcium sensitizing properties. *J. Med. Chem.* **1992**,

35, 163–172.

55. Singh, B.; Bacon, E. R.; Robinson, S.; Fritz, R. K.; Lesher, G. Y.; Kumar, V.; Dority, J. A.; Reuman, M.; Kuo, G. H.; Eissenstat, M. A.; Pagani, E. D.; Bode, D. C.; Bentley, R. G.; Connell, M. J.; Hamel, L. T.; Silver, P. J. Novel cAMP PDE-III inhibitors: imidazo[4,5-*b*]pyridin-2(3*H*)-ones and thiazolo[4,5-*b*]pyridin-2(3*H*)-ones and their analogs. *J. Med. Chem.* **1994**, *37*, 248–254.

56. Griffin, J. F.; Larson, D. L.; Portoghese, P. S. Crystal structures of alpha- and beta-funaltrexamine: conformational requirement of the fumaramate moiety in the irreversible blockage of mu opioid receptors. *J. Med. Chem.* **1986**, *29*, 778–783.

57. Jones, G.; Willett, P.; Glen, R. C.; Leach, A. R.; Taylor, R. Development and validation of a genetic algorithm for flexible docking. *J. Mol. Biol.* **1997**, *267*, 727–748.

58. Huang, W.; Manglik, A.; Venkatakrishnan, A. J.; Laeremans, T.; Feinberg, E. N.; Sanborn, A. L.; Kato, H. E.; Livingston, K. E.; Thorsen, T. S.; Kling, R. C.; Granier, S.; Gmeiner, P.; Husbands, S. M.; Traynor, J. R.; Weis, W. I.; Steyaert, J.; Dror, R. O.; Kobilka, B. K. Structural insights into mu-opioid receptor activation. *Nature* **2015**, *524*, 315–321.

59. Manglik, A.; Kruse, A. C.; Kobilka, T. S.; Thian, F. S.; Mathiesen, J. M.; Sunahara, R. K.; Pardo, L.; Weis, W. I.; Kobilka, B. K.; Granier, S. Crystal structure of the mu-opioid receptor bound to a morphinan antagonist. *Nature* **2012**, *485*, 321–326.

60. Ballesteros, J. A.; Weinstein, H. Integrated methods for the construction of three-dimensional models and computational probing of structure-function relations in G protein-coupled receptors. *Methods in Neuroscience*; Academic Press: San Diego, 1995; pp 366–428.

61. Rahm, M.; Hoffmann, R.; Ashcroft, N. W. Atomic and ionic radii of elements 1-96. *Chemistry* **2016**, *22*, 14625–14632.

62. Wu, H.; Wacker, D.; Mileni, M.; Katritch, V.; Han, G. W.; Vardy, E.; Liu, W.; Thompson, A. A.; Huang, X. P.; Carroll, F. I.; Mascarella, S. W.; Westkaemper, R. B.; Mosier, P. D.; Roth, B. L.; Cherezov, V.; Stevens, R. C. Structure of the human kappa-opioid receptor in complex with JDTic. *Nature* **2012**, *485*, 327–332.

63. Granier, S.; Manglik, A.; Kruse, A. C.; Kobilka, T. S.; Thian, F. S.; Weis, W. I.; Kobilka, B. K. Structure of the delta-opioid receptor bound to naltrindole. *Nature* **2012**, *485*, 400–404.

64. Che, T.; Majumdar, S.; Zaidi, S. A.; Ondachi, P.; McCorvy, J. D.; Wang, S.; Mosier, P. D.; Uprety, R.; Vardy, E.; Krumm, B. E.; Han, G. W.; Lee, M. Y.; Pardon, E.; Steyaert, J.; Huang, X. P.; Strachan, R. T.; Tribo, A. R.; Pasternak, G. W.; Carroll, F. I.; Stevens, R. C.; Cherezov, V.; Katritch, V.; Wacker, D.; Roth, B. L. Structure of the nanobody-stabilized active state of the kappa opioid receptor. *Cell* **2018**, *172*, 55–67.

65. Coward, P.; Chan, S. D.; Wada, H. G.; Humphries, G. M.; Conklin, B. R. Chimeric G proteins allow a high-throughput signaling assay of G_i-coupled receptors. *Anal. Biochem.* **1999**, *270*, 242–248.

66. Obeng, S.; Yuan, Y.; Jali, A. M.; Selley, D. E.; Zhang, Y. In vitro and in vivo functional profile characterization of 17-cyclopropylmethyl-3,14*β*-dihydroxy-4,5*α*-epoxy-6*α*-(isoquinoline-3-carboxamido) morphinan (NAQ) as a low efficacy mu opioid receptor modulator. *Eur. J. Pharmacol.* **2018**, *827*, 32–40.

67. Kowal, D., Zhang, J., Nawoschik, S., Ochalski, R., Vlattas, A., Shan, Q., Schechter, L., and Dunlop, J. The C-terminus of Gi family G-proteins as a determinant of 5-HT(1A) receptor coupling. *Biochem. Biophys. Res. Commun.* **2002**, *294*, 655–659.

68. Al-Hasani, R.; Bruchas, M. R. Molecular mechanisms of opioid receptor-dependent signaling and behavior. *Anesthesiology* **2011**, *115*, 1363–1381.

69. Charney, D. S.; Redmond, D. E., Jr.; Galloway, M. P.; Kleber, H. D.; Heninger, G. R.; Murberg, M.; Roth, R. H. Naltrexone precipitated opiate withdrawal in methadone addicted human subjects: evidence for noradrenergic hyperactivity. *Life Sci.* **1984**, *35*, 1263–1272.

70. Resnick, R. B.; Kestenbaum, R. S.; Washton, A.; Poole, D. Naloxone-precipitated withdrawal: a method for rapid induction onto naltrexone. *Clin. Pharmacol. Ther.* **1977**, *21*, 409–413.

71. Mitra, P.; Venitz, J.; Yuan, Y.; Zhang, Y.; Gerk, P. M. Preclinical disposition (in vitro) of novel mu-opioid receptor selective antagonists. *Drug Metab. Dispos.* **2011**, *39*, 1589–1596.

72. Yuan, Y.; Stevens, D. L.; Braithwaite, A.; Scoggins, K. L.; Bilsky, E. J.; Akbarali, H. I.; Dewey, W. L.; Zhang, Y. 6*β*-*N*-heterocyclic substituted naltrexamine derivative NAP as a potential lead to develop peripheral mu opioid receptor selective antagonists. *Bioorg. Med. Chem. Lett.* **2012**, 22, 4731–4734.

73. Cheng, Y.; Prusoff, W. H. Relationship between the inhibition constant (K_i) and the concentration of inhibitor which causes 50 percent inhibition (IC_{50}) of an enzymatic reaction. *Biochem. Pharmacol.* **1973**, *22*, 3099–3108.

Table of Contents graphic

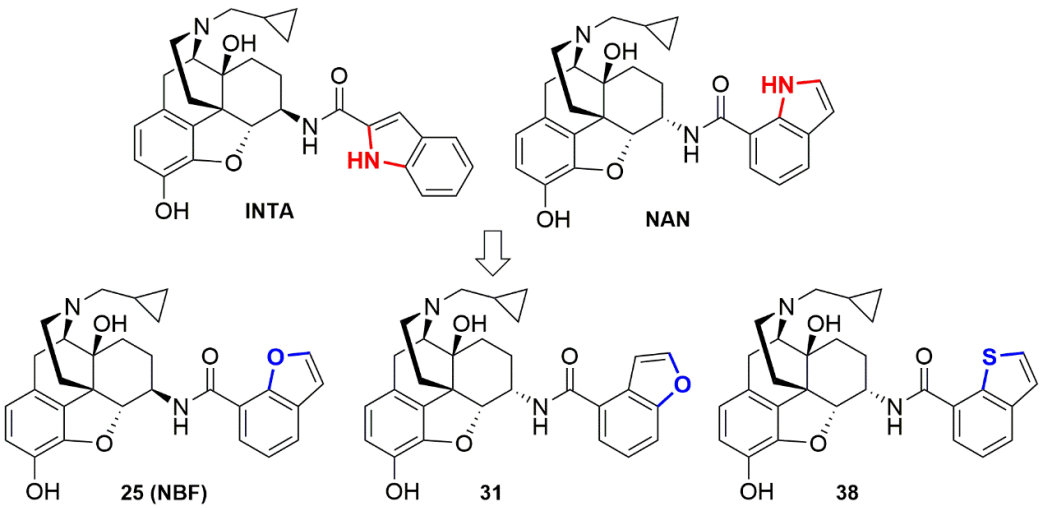

Bivalent bioisosteric replacements lead to 7 to 12-fold enhanced antagonist potency.